AFAPL-TR-72-28

AN INVESTIGATION OF SCUFFING CONDUCTED ON THE AFAPL DISK TESTER

H. J. Carper
E. L. Anderson
P. M. Ku

Southwest Research Institute

TECHNICAL REPORT AFAPL-TR-72-28

June 1972

Air Force Aero Propulsion Laboratory
Air Force Systems Command
Wright-Patterson Air Force Base, Ohio

NOTICE

When Government drawings, specifications, or other data are used for any purpose other than in connection with a definitely related Government procurement operation, the United States Government thereby incurs no responsibility, nor any obligation whatsoever; and the fact that the Government may have formulated, furnished, or in any way supplied the said drawings, specifications, or other data, is not to be regarded by implication or otherwise as in any manner licensing the holder or any other person or corporation, or conveying any rights or permission to manufacture, use, or sell any patented invention that may in any way be related thereto.

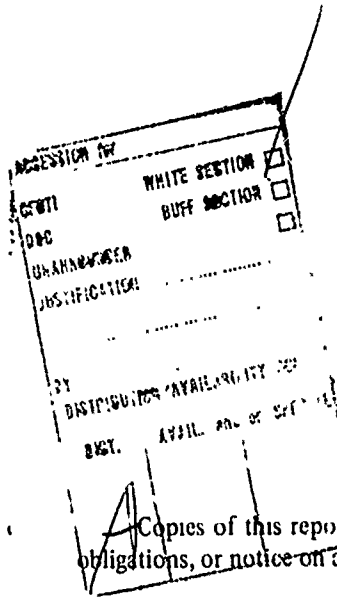

Copies of this report should not be returned unless return is required by security considerations, contractual obligations, or notice on a specific document.

UNCLASSIFIED
Security Classification

DOCUMENT CONTROL DATA - R & D

(Security classification of title, body of abstract and indexing annotation must be entered when the overall report is classified)

1. ORIGINATING ACTIVITY (Corporate author)	2a. REPORT SECURITY CLASSIFICATION
Southwest Research Institute 8500 Culebra Road San Antonio, Texas 78284	Unclassified 2b. GROUP

3. REPORT TITLE

AN INVESTIGATION OF SCUFFING CONDUCTED ON THE AFAPL DISK TESTER

4. DESCRIPTIVE NOTES (Type of report and inclusive dates)

Phase Report, April 1, 1971 through January 31, 1972

5. AUTHOR(S) (First name, middle initial, last name)

Carper, H. J., Anderson, E.L. and Ku, P. M.

6. REPORT DATE	7a. TOTAL NO. OF PAGES	7b. NO. OF REFS
June 1972	33 plus 9 Preliminaries	4

8a. CONTRACT OR GRANT NO.	9a. ORIGINATOR'S REPORT NUMBER(S)
F33615-69-C-1295	
b. PROJECT NO. 3048	RS-586
c. Task No. 304806	9b. OTHER REPORT NO(S) (Any other numbers that may be assigned this report)
d.	AFAPL-TR-72-28

10. DISTRIBUTION STATEMENT

Approved for public release; distribution unlimited

11. SUPPLEMENTARY NOTES	12. SPONSORING MILITARY ACTIVITY
	Air Force Aero Propulsion Laboratory Air Force Systems Command Wright-Patterson Air Force Base, Ohio 45433

13. ABSTRACT

This report presents the results of scuffing studies conducted on the AFAPL disk tester developed earlier. A total of 90 tests were conducted using AMS 6260 CEVM steel disks and a MIL-L-7808G lubricant at various combinations of sliding and sum velocities, at two lubricant jet temperatures, with two methods of driving the test disks, and in air and inert environments. The load-carrying capacity is seen to decrease with increasing sliding velocity, increase with increasing sum velocity, decrease with increasing lubricant jet temperature, decrease with belted as against unbelted drive, and decrease in the presence of an inert environment. The variations of the critical temperature, the minimum lubricant film thickness ratio at failure, and the friction coefficient at failure with respect to the variables investigated are presented and discussed.

DD FORM 1 NOV 65 1473

UNCLASSIFIED
Security Classification

14. KEY WORDS	LINK A		LINK B		LINK C	
	ROLE	WT	ROLE	WT	ROLE	WT
Load-Carrying Capacity, Gear						
Scuffing, Gear						
Test, Disk						
Tester, AFAPL Disk						

AN INVESTIGATION OF SCUFFING CONDUCTED ON THE AFAPL DISK TESTER

H. J. Carper
E. L. Anderson
P. M. Ku

FOREWORD

This report was prepared by Southwest Research Institute, 8500 Culebra Road, San Antonio, Texas, under Contract F33615-69-C-1295. The contract was initiated under Project No. 3048, "Fuels, Lubrication, and Hazards," Task No. 304806, "Aerospace Lubrication." The work was administered by the Lubrication Branch, Air Force Aero Propulsion Laboratory, Air Force Systems Command, Wright-Patterson Air Force Base, Ohio. The project engineers were Messrs. E.A. Lake and H.A. Smith (AFAPL/SFL).

The report covers one phase of work performed under the subject contract in the period of April 1, 1971 through January 31, 1972. This report was submitted by the authors in March 1972.

The contractor's report number is RS-586.

Publication of this report does not constitute Air Force approval of the report's findings or conclusions. It is published only for the exchange and stimulation of ideas.

K.L. Berkey
Chief, Lubrication Branch
Fuels and Lubrication Division
Air Force Aero Propulsion Laboratory

ABSTRACT

This report presents the results of scuffing studies conducted on the AFAPL disk tester developed earlier. A total of 90 tests were conducted using AMS 6260 CEVM steel disks and a MIL-L-7808G lubricant at various combinations of sliding and sum velocities, at two lubricant jet temperatures, with two methods of driving the test disks, and in air and inert environments. The load-carrying capacity is seen to decrease with increasing sliding velocity, increase with increasing sum velocity, decrease with increasing lubricant jet temperature, decrease with belted as against unbelted drive, and decrease in the presence of an inert environment. The variations of the critical temperature, the minimum lubricant film thickness ratio at failure, and the friction coefficient at failure with respect to the variables investigated are presented and discussed.

TABLE OF CONTENTS

LIST OF ILLUSTRATIONS

LIST OF ILLUSTRATIONS (Cont'd)

LIST OF TABLES

LIST OF SYMBOLS

a	major axis semiwidth of conjunction ellipse, in.
b	minor axis semiwidth of conjunction ellipse, in.
E	Young's modulus, psi (E_1 for upper disk, E_2 for lower disk)
E^*	equivalent Young's modulus, psi $= 2[(1-\nu_1^2)/E_1 + (1-\nu_2^2)/E_2]^{-1}$
f	disk friction coefficient = T_f/rP
f_f	disk friction coefficient at scuffing failure
h_m	minimum elastohydrodynamic film thickness, μin.
h_{mf}	minimum elastohydrodynamic film thickness at scuffing failure, μin.
M	ratio of sliding velocity to sum velocity = V_s/V_t
mm	metal monitor reading
N	rotational speed of disks, rpm (N_1 for upper disk, N_2 for lower disk)
P	disk load, lb
P_f	disk load at scuffing failure, lb
r	disk radius, in. (r_1 for upper disk, r_2 for lower disk)
R	equivalent radius of disk pair, in. = $r_1 r_2/(r_1 + r_2)$
S	ratio of disk rotational speeds = N_1/N_2
ΔT	conjunction temperature rise, °F
T_{cr}	critical temperature, °F
T_f	disk friction torque, in.-lb
T_j	lubricant jet temperature, °F
T_m	machine loss torque, in.-lb (T_{m1} for upper shaft, T_{m2} for lower shaft)
T_p	thermocouple probe temperature, °F (T_{p1} for probe riding on upper disk, T_{p2} for probe riding on lower disk)
T_r	reaction torque, in.-lb (T_{r1} for upper shaft, T_{r2} for lower shaft)
T_s	disk surface temperature, °F (T_{s1} for upper disk, T_{s2} for lower disk)

LIST OF SYMBOLS (Cont'd)

V	peripheral velocity of disk surface, ips (V_1 for upper disk, V_2 for lower disk)
V_s	sliding velocity, ips = $V_1 - V_2$
V_t	sum velocity, ips = $V_1 + V_2$
w_e	equivalent load, ppi
α_o	pressure-viscosity coefficient of lubricant at conjunction inlet temperature and atmospheric pressure, psi^{-1}
β	Blok's thermal coefficient, lb/°F-in.-$sec^{1/2}$
δ	composite surface roughness of a pair of disks, μin. CLA = $\delta_1 + \delta_2$ (δ_i for initial, δ_a for after break-in, δ_f for after failure)
δ_1	composite surface roughness of upper disk, μin. CLA = $(\delta_{x1} + \delta_{y1})/2$
δ_2	composite surface roughness of lower disk, μin. CLA = $(\delta_{x2} + \delta_{y2})/2$
δ_x	surface roughness of disk measured in direction of motion, μin. CLA
δ_y	surface roughness of disk measured perpendicular to direction of motion, μin. CLA
Λ_m	minimum lubricant film thickness ratio = h_m/δ_a
Λ_{mf}	minimum lubricant film thickness ratio at failure = h_{mf}/δ_a
μ_o	lubricant viscosity at conjunction inlet temperature and atmospheric pressure, cp
μ_j	lubricant viscosity at lubricant jet temperature and atmospheric pressure, cp
ν	Poisson's ratio of disk material (ν_1 for upper disk, ν_2 for lower disk)
σ	stress, psi ($\bar{\sigma}$ for mean stress, σ_m for maximum stress)

SECTION I

INTRODUCTION

1. General

In a previous report,[1]* the authors described in detail a disk tester for gear lubrication research, designed and developed by Southwest Research Institute (SwRI) for the Air Force Aero Propulsion Laboratory (AFAPL). Also included in that report were the results of some preliminary scuffing tests conducted using the new tester. These tests were considered preliminary because operating procedures were being developed for the tester as data were being collected, and the machine operator was gaining experience in test control and scuffing failure detection. In addition, the torquemeters used in the earlier tests had a capacity that was too large compared with the reaction torques that were being observed on the disk shafts. These torquemeters have since been replaced with ones of smaller capacity. As will be seen later, the new torquemeters have considerably improved the accuracy in the determination of the disk friction.

This report presents the results of a program conducted using the AFAPL disk tester to determine the effects of sliding velocity, sum velocity, lubricant jet temperature, and environmental atmosphere on the scuffing phenomena of disks made from a typical gear steel (AMS 6260) and lubricated with a common synthetic gas turbine engine lubricant (MIL-L-7808G). In addition, the results of new machine loss and temperature calibrations used in the calculation of the test results are also presented.

2. Experimental and Analytical Approach

The philosophy of SwRI's approach to the scuffing problem has been dealt with previously.[1] Briefly, it is felt that even though the load-carrying capacity is ultimately the quantity of most practical interest to designers, it is not a fundamental quantity that governs the scuffing process. This is evident from the lack of direct correlation of the load-carrying capacity data from the various test devices and test methods. To find a more rational means of lubricant selection and gear performance prediction, scuffing studies at SwRI have concentrated on the evaluation of more fundamental approaches, such as the critical temperature hypothesis,[2,3] the elastohydrodynamic (EHD) film thickness theory,[4] and other possible criteria.

With appropriate instrumentation on the disk tester, the quantities necessary for input to the expressions for critical temperature and minimum EHD film thickness are measured and these two quantities calculated. Then the behavior of these quantities with such operating conditions as speed, lubricant temperature, and environmental atmosphere, etc., can be examined and evaluated.

The relationships used for the calculation of critical temperature and EHD film thickness were presented in detail in the earlier report.[1]

---

*Superscript numbers in parentheses refer to the list of References at the end of this report.

SECTION II

TEST APPARATUS

1. General

A complete description of the AFAPL disk tester, together with test disk geometry, the instrumentation, the calibration and operating procedures, was presented in Reference 1.

Two major changes in the test equipment were introduced during this reporting period. One was the replacement of the two 2000-in.-lb torquemeters with two 500-in.-lb torquemeters. The 500-in.-lb torquemeter capacity was selected so as to improve the accuracy in the measurement of the reaction torques on the two shafts, from which the disk friction torque must be derived. The reaction torques encountered in the program ranged from approximately 25 to 250 in.-lb. The 500-in.-lb capacity was the smallest capacity available that would satisfy the other application requirements.

The other change was the provision for an alternative drive system, which is described in the following section.

2. Unbelted and Belted Drive Systems

As originally designed, the upper disk of the AFAPL disk tester is driven by a motor, and the lower disk is connected to a motor/brake unit that can hold the lower disk at any speed equal to or different from that of the upper disk. With independent, stepless speed controls on the motor and motor/brake units, any combination of sliding and sum velocities can readily be obtained. This is a highly desirable feature for a research apparatus intended to cover a wide range of sliding to sum velocity ratios.

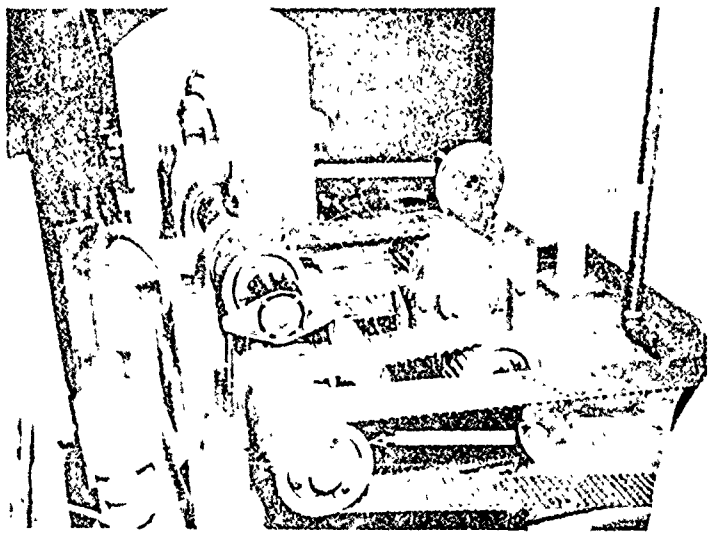

FIGURE 1. THE BELTED DRIVE SYSTEM

A more conventional type of drive system is one in which the two disk shafts are connected by either phase gears, or belts and pulleys. With this arrangement, the sliding to sum velocity ratio is fixed. Thus, each time a different sliding to sum velocity ratio is desired, the phase gear ratio or pulley diameter ratio must be changed. This type of drive system is less versatile; however, it is the type more commonly used in gear lubrication and scuffing research.

In order to determine whether there would be a difference in results if the disk tester were operated in the conventional as compared with the intended manner, a pulley and timing belt arrangement was devised to "gear" the two shafts together. Figure 1 is a photograph of this belted drive system. Through the belting arrangement shown, a motor drives the lower shaft which, in turn, drives a direction-reversing gearbox with a 2:1 gear ratio. The pulley on the output side of the gearbox then drives the upper shaft. By changing the pulley sizes various combinations of sliding and sum velocities can be obtained. The quite interesting difference in results obtained by operating the tester in these two ways is discussed later.

SECTION III

IMPROVED CALIBRATION RESULTS

1. Improved Machine Loss Calibration

After the new torquemeters were installed, a second machine loss calibration was conducted using lubricant O-67-22 (MIL-L-7808G) and the procedure previously outlined.[1] The results were in general agreement with the previous ones obtained using the less sensitive torquemeters in that the relationship between machine-loss torque and disk load was linear at constant shaft speed and lubricant viscosity. Also, a linear relationship between machine-loss torque and shaft speed at constant load was observed.

The machine loss was derived by two techniques which, for convenience, will be referred to hereafter as the old and new techniques.

Old Technique. It was previously shown[1] that for the upper disk shaft

$$T_{r1} = T_f + T_{m1} \tag{1}$$

and for the lower disk shaft

$$T_{r2} = T_f - T_{m2} \tag{2}$$

where

T_f – disk friction torque, in.-lb

T_{r1} – reaction torque indicated by torquemeter on the upper shaft, in.-lb

T_{r2} – reaction torque indicated by torquemeter on the lower shaft, in.-lb

T_{m1} – machine-loss torque for upper shaft, in.-lb

T_{m2} – machine-loss torque for lower shaft, in.-lb

In Eqs. (1) and (2), T_f is obviously the same under any condition of operation. Further, if the calibration is performed with the two shafts operating at precisely or approximately the same speed, then for identical bearings and shafts

$$T_m = T_{m1} = T_{m2} \tag{3}$$

where T_m is the machine-loss torque, in.-lb, at the specific speed, load, and other operating conditions at which the calibration is performed. With this assumption, subtracting Eq. (2) from Eq. (1) yields

$$T_m = \frac{T_{r1} - T_{r2}}{2} \tag{4}$$

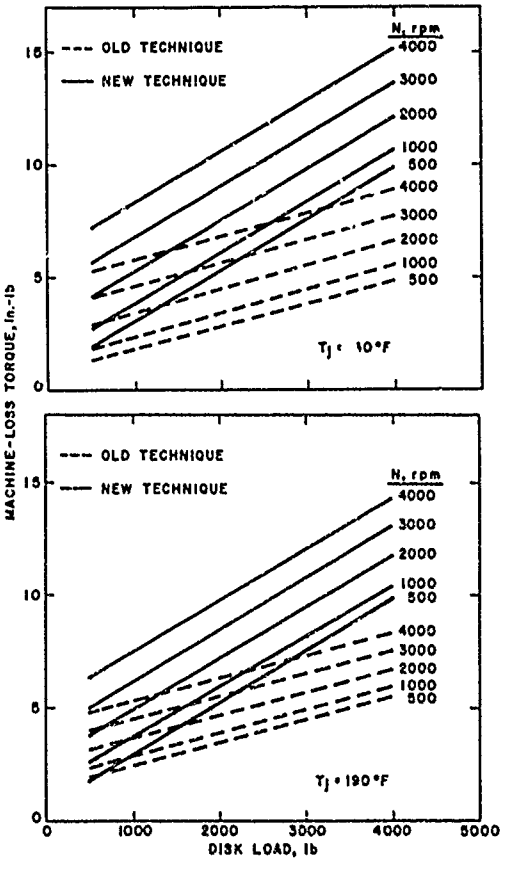

FIGURE 2. COMPARISON OF MACHINE LOSS CALIBRATION METHODS USING LUBRICANT O-67-22

Such a calibration was performed with lubricant O-67-22 and the new torquemeters. The results are shown as dashed curves in Figure 2, in which the data points have been omitted for the sake of clarity. As mentioned previously, these results are in general agreement with those reported in Reference 1.

New Technique. When the data reduction on the scuffing test results began, differences were noted in the two values of the disk friction coefficient at failure derived from the two torquemeter readings. A difference was also observed in the preliminary scuffing studies, but this was attributed to the fact that the first machine loss calibration contained some inaccuracies due to the less sensitive torquemeters.(1)

In order to bring the two friction coefficients into better agreement, a different procedure was tried. This procedure involved first assuming a functional relationship for the machine-loss torque in terms of speed, load, lubricant viscosity, and undetermined constants. Then, using the fact that the coefficients of friction as derived from the two torquemeters must, by definition, be equal, equations were developed that allowed the constants in the machine loss equation to be calculated from experimental data.

With the new technique, it is no longer necessary to operate the two shafts at approximately the same speed. Rather, the shafts may operate at any speeds, as in the actual scuffing tests. Thus, the method has the advantage that the torquemeter readings obtained during scuffing tests can be used to determine the constants in the machine loss equation. These larger readings are more accurate than the relatively small readings obtained in determining the machine-loss torques by the old technique.

As can be seen in Figure 2, by the old technique it was found that the machine-loss torque varied linearly with load at constant speed and lubricant viscosity. It can also be seen that, at constant load and lubricant viscosity, the variation of machine-loss torque with speed is approximately linear. Based on these two observations, and being guided by the results from the old technique with respect to the effect of viscosity, a general expression for the machine-loss torque may be written as

$$T_m = aP + bN\mu_j^c \tag{5}$$

where

T_m – machine-loss torque for one shaft, in.-lb

P – disk load, lb

N – shaft speed, rpm

μ_j – lubricant viscosity at T_j and atmospheric pressure, cp

a,b,c -- fitting constants

Since the two shafts are identical and are mounted in identical bearings, it is assumed that Eq. (5) can be applied to either shaft under any set of operating conditions. Thus the results obtained in the actual scuffing tests can be employed directly to determine the fitting constants a, b, and c. The details of the procedure are given in Appendix I; the resulting equation for the machine-loss torque is

$$T_m = 0.0023P + 0.000968N\mu_j^{0.23} \tag{6}$$

where

T_m machine-loss torque, in.-lb (T_{m1} for upper shaft, T_{m2} for lower shaft)

P - disk load, lb

N – disk speed, rpm (either N_1 or N_2 depending on whether the upper or the lower disk shaft is under consideration)

μ_j - lubricant viscosity at T_j and atmospheric pressure, cp

The calculated results from Eq. (6) are shown as solid curves in Figure 2, for comparison with the results derived from the old technique shown as dashed curves. Note that the new technique predicts higher machine-loss torques than the old technique, particularly at high disk loads.

The discrepancy of results from the old and new techniques underscores the basic difficulty with all types of disk testers for which the disk friction must be derived from the reaction torques measured on the shafts which, by necessity, include the contributions of the support bearings. It is a moot question which technique gives a better prediction of the machine-loss torque. The crucial question is which technique gives a better correlation of the disk friction coefficient. Obviously, since the disk friction coefficient must, by definition, be the same for the upper disk as for the lower disk, then the new technique, which recognizes this fact, is to be preferred.

Of course, in the derivation of the "smoothed" data presented in Figure 2, experimental errors in obtaining the raw data and the subsequent treatment of the raw data all tend to introduce some uncertainties. In the last analysis, it does not matter which technique gives the "correct" machine-loss torque, but rather which technique gives the "correct" disk friction coefficient which nature demands to be equal on the basis of either the upper or lower disk. From extensive analysis and comparison of all of the scuffing test results available from the AFAPL disk tester over the entire range of variables employed to date, it has been found that the two disk friction coefficients at failure derived from machine-loss data obtained by the old technique differ in most cases by approximately 10 percent and occasionally by as much as 20 percent. On the other hand, by using machine-loss data obtained by the new technique, the two friction coefficients usually agree to within 5 percent and only in rare instances to about 10 percent. On the basis of these findings, it is concluded that the new technique gives more plausible results.

2. Simultaneous Temperature Measurements in Upper and Lower Disks

As explained previously,[1] the AFAPL disk tester is equipped with a thermocouple probe located in the center plane of the disks 1/3 in. ahead of the center of the conjunction. This thermocouple probe may be made to suspend freely without touching either disk or to ride with a slight pressure on one of the disks. Due to the complex oil flow and heat transfer conditions prevalent at this vicinity, the temperature across the oil film is generally not uniform, and the probe reading with the probe touching the upper (or faster) disk is always higher than the reading with the probe touching the lower disk sometimes by as much as 30°F. In any case, regardless of the probe's position, it does not read directly the surface temperature of either disk.

In order to derive the surface temperature, T_s, of a disk from the probe temperature, T_p, with the probe touching that disk, the relationship between the disk surface temperature and the corresponding probe temperature must be known. Such a relationship can only be established by calibration,[1] which involves instrumenting a disk with embedded thermocouples and taking simultaneous readings from the embedded thermocouples and the thermocouple probe riding on the same disk. As mentioned previously, however, the thermocouple probe always reads higher when riding on the upper disk than when riding on the lower disk. The question then arises as to whether the T_s vs T_p relationship is or is not the same for the upper and lower disks. Indeed, if this relationship were the same for both disks, then the surface temperature of the upper (or faster) disk must necessarily be higher than that of the lower disk. This would then yield two calculated critical temperatures, which would be difficult to interpret.

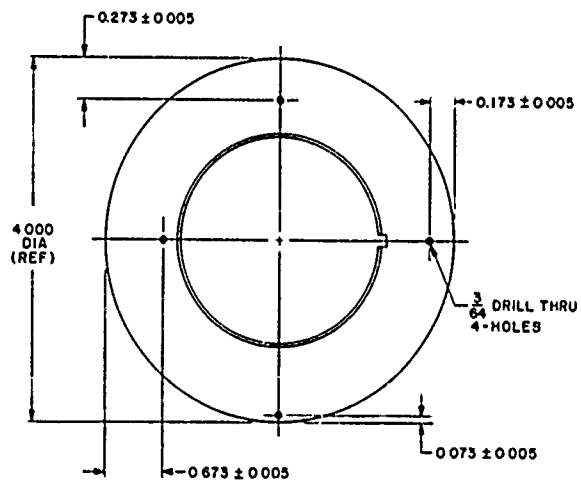

FIGURE 3. THERMOCOUPLE HOLE LOCATIONS IN TEST DISK

In order to determine if the two surface temperatures were different, simultaneous temperature measurements were made on both the upper and lower disks. For this work, the holes drilled in the calibration disks were relocated as shown in Figure 3. As can be seen by comparing this figure with Figure 14 in Reference 1, a hole was placed between the first and second original holes to allow a more accurate determination of the gradient near the surface, hence a more accurate extrapolation to the surface temperature.

Both the upper and lower disks were instrumented with embedded thermocouples, and two

identical mercury slip rings were installed on the two shafts to connect the embedded thermocouples to the temperature recorder. The disk tester was then operated with lubricant O-67-22 at various conditions of speed and load, and the temperatures at three different radial positions (as limited by the capacity of the mercury slip rings) in the upper and lower disks were recorded simultaneously. Also, at each condition, the thermocouple probe readings with the probe riding on the upper and lower disks were both obtained. This procedure was carried out at T_j = 140° and 190°F, but more extensively at T_j = 190°F since the majority of the scuffing tests were to be conducted at the higher lubricant jet temperature.

Figure 4 shows typical temperature distributions in the disks for one set of speed conditions, where V_s = 300 ips and V_t = 200 ips. Figure 4a was obtained with T_j = 140°F, while Figure 4b was obtained with T_j = 190°F. The three curves were generated by using three different values of disk load. The surface temperature was obtained by extrapolation of the embedded thermocouple temperatures, assuming a linear relationship between the disk temperature and the logarithm of the radial distance. This procedure has been used as a standard technique throughout all the calibration work. As shown in the figure, at each radial position there is little difference in the embedded thermocouple temperatures, which results in the extrapolated surface temperatures being nearly the same for both the upper and lower disks.

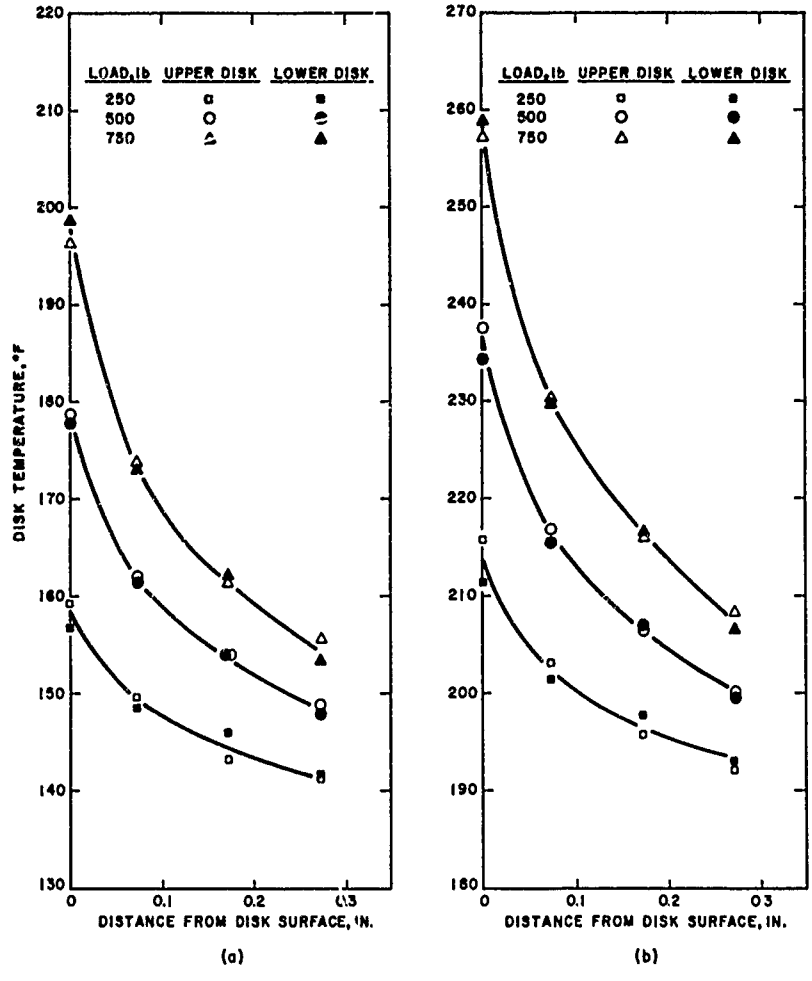

FIGURE 4. TYPICAL TEMPERATURE DISTRIBUTIONS IN TEST DISKS

Figure 5 shows all the results for T_j = 140°F, where the surface temperature for the upper disk is plotted against the surface temperature for the lower disk. As shown in the figure, data were obtained for three values of sliding to sum velocity ratio, M. The dashed line shown in the figure is where $T_{s_1} = T_{s_2}$, and, as can be seen, the surface temperatures agree well with this relationship. It will be noted that the disk surface temperatures do not extend quite as high as some of the surface temperatures obtained in the scuffing tests. This is because the maximum load was intentionally kept low in order not to scuff the calibration disks, which are extremely time-consuming to make and were limited in quantity. In about half of the scuffing tests, at

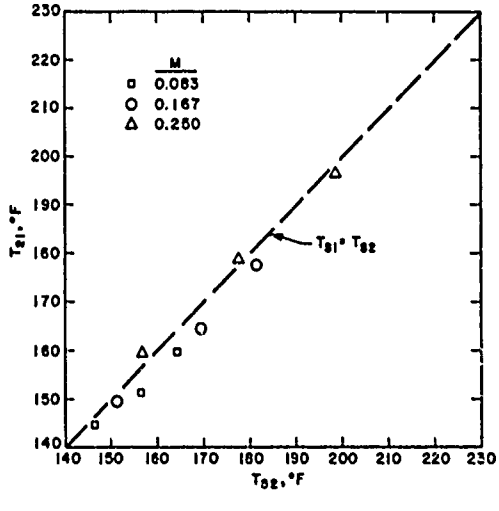

FIGURE 5. COMPARISON OF SURFACE TEMPERATURES OF TEST DISKS AT T_j = 140°F

T_j = 140°F, the surface temperature was approximately 200°F or lower, which was the highest temperature observed in the simultaneous temperature measurements.

Figure 6 shows the relationship between the extrapolated disk surface temperature and the corresponding thermocouple probe temperature for the same conditions presented in Figure 5. It is apparent that, although the surface temperatures are nearly equal as shown in Figure 5, the thermocouple probe temperatures are not the same for the two disks. For a given surface temperature, the thermocouple probe temperature on the upper disk is always higher than that on the lower disk.

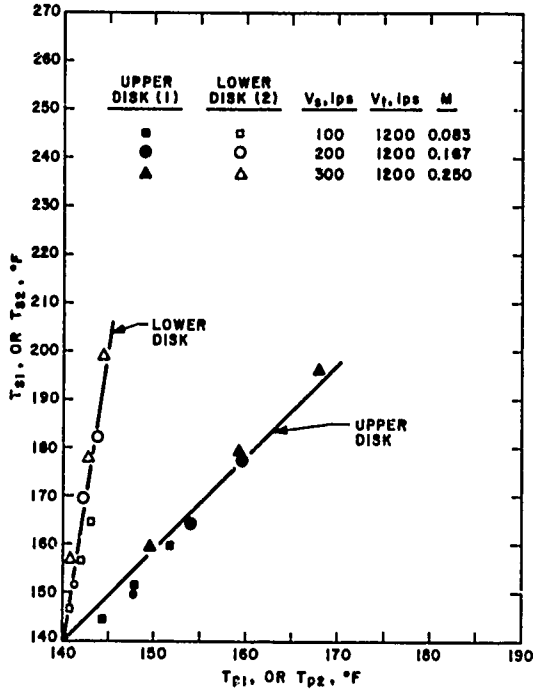

FIGURE 6. RELATIONSHIP BETWEEN DISK SURFACE TEMPERATURE AND UPPER AND LOWER THERMOCOUPLE PROBE TEMPERATURES FOR T_j = 140°F

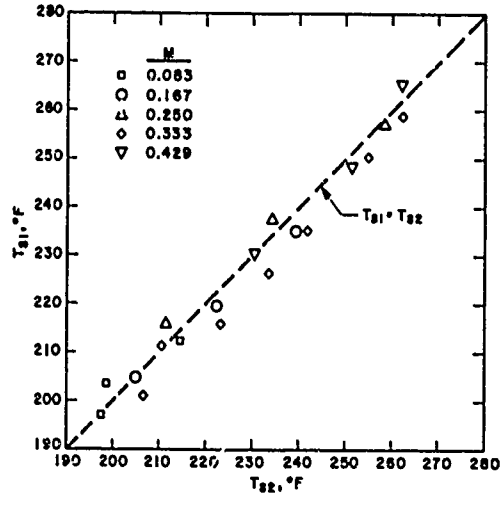

FIGURE 7. COMPARISON OF SURFACE TEMPERATURES OF TEST DISKS AT T_j = 190°F

Figure 7 shows the simultaneous surface temperature determinations for T_j = 190°F. The data were obtained for the embedded thermocouple temperatures at five values of M. The two highest ratios were identical to those used in many of the scuffing tests. As can be seen, the two surface temperatures are in good agreement over the whole range. The highest extrapolated surface temperature obtained was about 265°F, which is as high as the surface temperature at scuffing for the majority of the tests conducted at T_j = 190°F.

The relationship between the extrapolated disk surface temperatures presented in Figure 7 and the corresponding thermocouple probe temperatures is shown in Figure 8. Similar to the case where T_j = 140°F, the thermocouple probe temperatures are not the same for the two disks. Likewise, for a given surface temperature, the probe temperature is always higher for the upper disk than for the lower disk.

It is clear from the above that with lubricated disks operated over a wide range of conditions, both the temperature distribution inside the two disks and the surface temperatures of the two disks are the same. However, the thermocouple probe temperatures with the probe touching the upper and lower disks are generally different. Therefore, the T_s vs T_p relationships for the two disks are different. In practice, either the upper or the lower disk may be employed to deduce disk surface temperature, provided the appropriate T_s vs T_p calibration is used.

3. Improved Temperature Calibration

Having ascertained that either the upper or the lower disk may be used to derive the disk surface temperature, a more detailed calibration was made with lubricant O-67-22 over a wide range of conditions. This calibration was made using the new calibration disks shown in Figure 3, and by careful placement of the thermocouple probe at a distance of 1/3 in. ahead of the center of the disk conjunction. Following the earlier practice[1], the lower disk was used as the basis for the temperature calibration.

Figure 9 shows the relationship between the extrapolated surface temperature, T_s, and the thermocouple probe temperature T_{p2}, for the two lubricant jet temperatures of 140° and 190°F. In contrast with the results previously

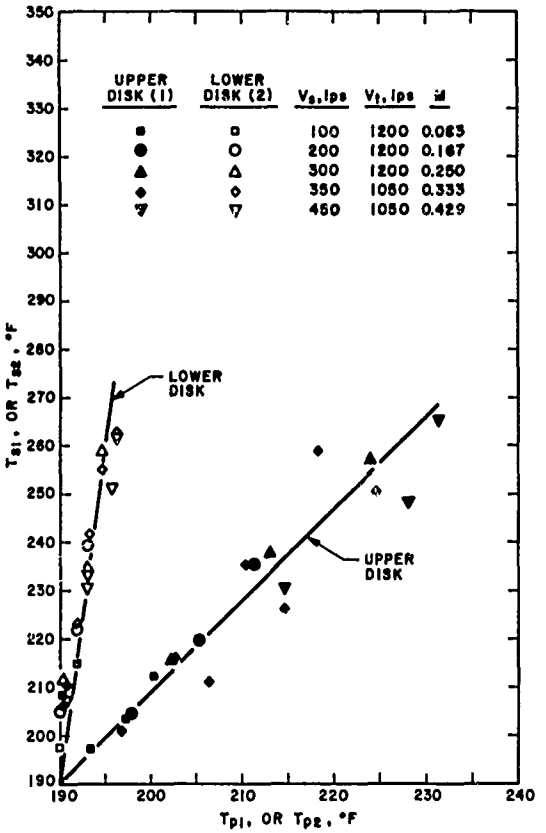

FIGURE 8. RELATIONSHIP BETWEEN DISK SURFACE TEMPERATURE AND UPPER AND LOWER THERMOCOUPLE PROBE TEMPERATURES FOR T_j = 190°F

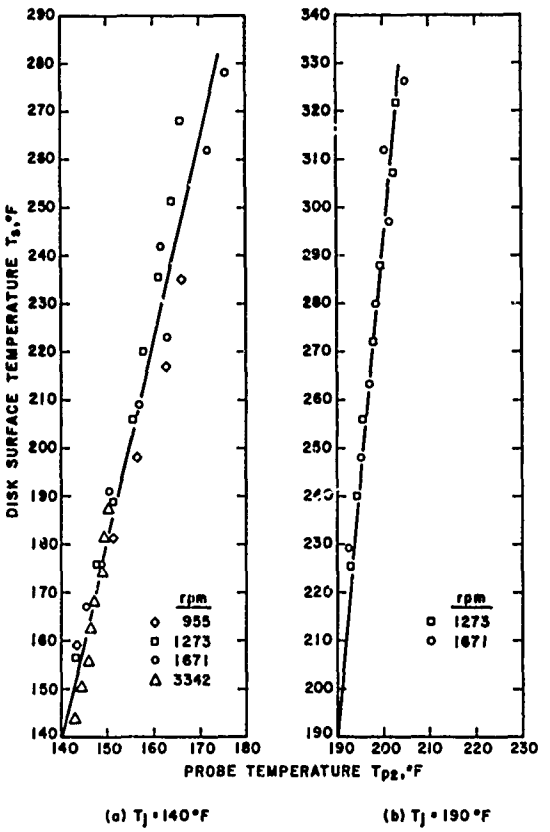

FIGURE 9. TEMPERATURE CALIBRATION FOR LUBRICANT O-67-22

obtained using lubricant BC[1], no speed effect was noted with lubricant O-67-22. That is, the T_s vs T_p relationship is a single curve for all disk speeds between 955 and 3342 rpm, and is linear. The slope of this curve is dependent upon the lubricant jet temperature, T_j. For T_j = 140°F, the extrapolated surface temperature is given by

$$T_s = 140 + 4.286\,(T_{p2} - 140) \tag{7}$$

and for T_j = 190°F

$$T_s = 190 + 10.000\,(T_{p2} - 190) \tag{8}$$

where

T_s – disk surface temperature, °F

T_{p2} – thermocouple probe temperature, °F (with probe riding on the lower disk)

It will be noted that the extrapolated surface temperature is extremely sensitive to changes in the thermocouple probe temperature. Thus, slight differences in the thermocouple probe temperature caused by factors such as probe installation or characteristics of the probe itself can introduce large errors in the predicted disk surface temperature, which is used to calculate critical temperature. For this reason, extreme precautions must be taken in the construction and installation of the thermocouple probes in order to ensure consistent conditions from test to test.

Figure 10 compares the single curve obtained with lubricant O-67-22 at $T_j = 140°F$, with the curves obtained using lubricant BC at the same temperature. As can be seen, there is considerable difference in the results for the two lubricants. This demonstrates the need for the temperature calibration to be conducted using the same lubricant that will be used in the actual scuffing tests. It is believed that the difference between the results can be explained by the fact that lubricant BC is about seven times as viscous as lubricant O-67-22 and thus results in a thicker lubricant film that affects the thermocouple probe temperature.

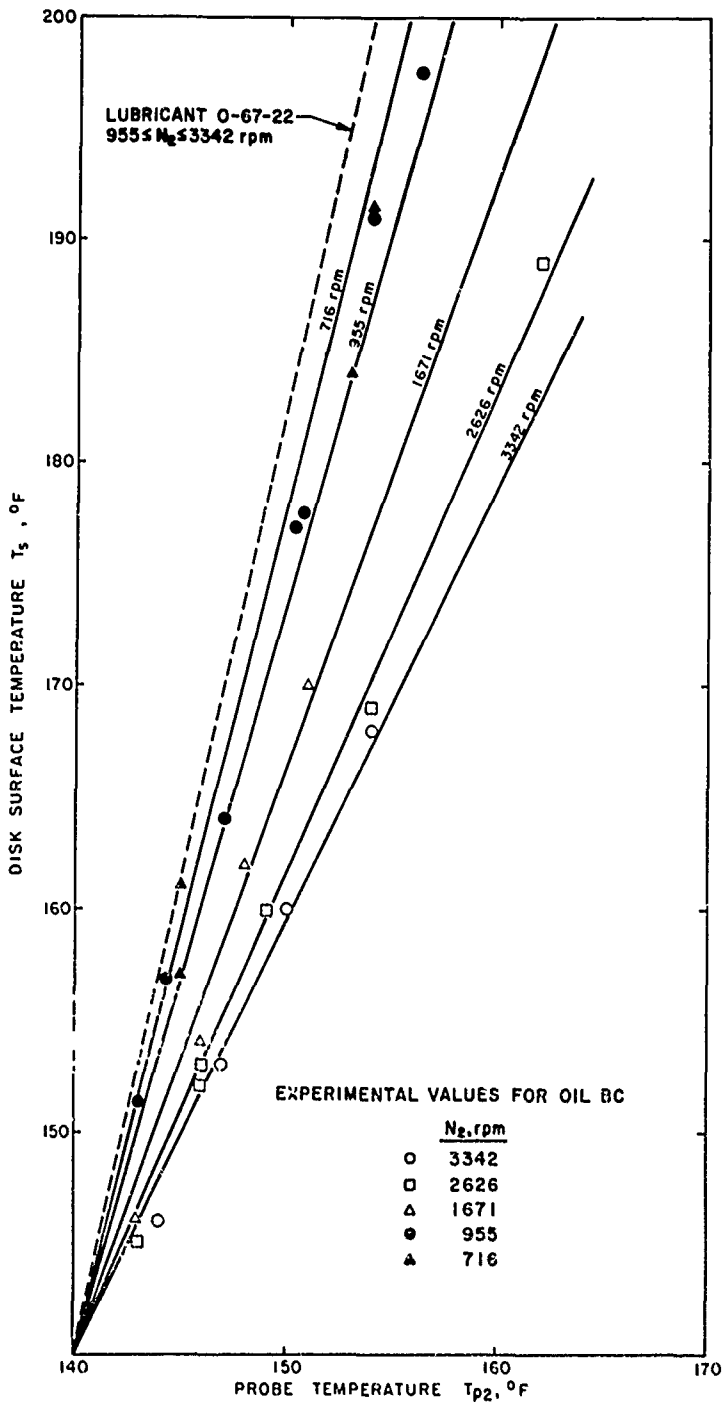

FIGURE 10. COMPARISON BETWEEN TEMPERATURE CALIBRATIONS USING LUBRICANTS BC AND O-67-22 AT $T_j = 140°F$

SECTION IV

RESULTS AND DISCUSSION

1. General

This section presents the experimental results of 90 scuffing tests conducted using disks operating at various combinations of sliding and sum velocities, with lubricant O-67-22 at two lubricant jet temperatures, and in air and nitrogen environments.

The test disks used in these experiments were fabricated from a single heat of AMS 6260 CEVM steel and represent the second batch of disks, Batch B, tested on the AFAPL disk tester. The first batch of disks, Batch A, also of AMS 6260 steel, were all tested at a lubricant jet temperature T_j = 140°F, but using three different lubricants. The results of these tests have been reported previously.(1)

The properties of lubricant O-67-22, a MIL-L-7808G lubricant, have been previously given in Reference 1.

The majority of the Batch B disks were tested at T_j = 190°F. However, some tests were conducted at T_j = 140°F for comparison with the results obtained with Batch A.

In the experience of SwRI with a very large number of disk tests, it has been noted that even with test disks made under very stringent control from a single heat of steel, and with tests conducted under the utmost care, replicate tests, as a rule, yield scuffing failure loads of considerable scatter, typically by a factor of 2 to 3. In the interest of statistical confidence, it was decided that, in testing with Batch B disks, 10 replicate tests should be conducted at each set of test conditions so that reliable averages would be obtained. This was done for 7 series of tests, thus accounting for 70 of the 90 tests conducted. It was then discovered that quite different test results were obtained by driving the test disks with the two alternate drive systems mentioned earlier. To explore the drive-system effect over the widest range of operating conditions possible with the remaining Batch B disks, it was necessary to run only 5 replicate tests for each of the 4 remaining series.

Before discussing the results, it will be helpful to summarize the test program by tabulating the test series numbers and the test conditions for each series. This is done in Table I. Seven test series, Series VIII to XIV, were conducted with the unbelted drive system. Series X, XI, and IX were intended to determine the effect of changing sliding velocity at constant sum velocity, while Series X, XII, and XIII were conducted to determine the effect of changing sum velocity at constant sliding velocity. Note that Series X is common to both groups of three series. Series VIII was conducted at T_j = 140°F, both for comparison with Batch A results and for comparison with Series IX to determine the effect of lubricant jet temperature, T_j. Series XIV was to be compared with Series XI for the effect of an inert environment.

TABLE I. SUMMARY OF TEST SERIES AND CONDITIONS WITH BATCH B AMS 6260 DISKS AND LUBRICANT O-67-22

Series	No. of tests	V_s, ips	V_t, ips	$M = V_s/V_t$	S	T_j, °F	Environment
Unbelted drive							
X	10	350	1050	0.333	2.0	190	Air
XI	10	450	1050	0.429	2.5	190	Air
IX	10	630	1050	0.600	4.0	190	Air
X	10	350	1050	0.333	2.0	190	Air
XII	10	350	817	0.429	2.5	190	Air
XIII	10	350	583	0.600	4.0	190	Air
VIII	10	630	1050	0.600	4.0	140	Air
XIV	10	450	1050	0.429	2.5	190	Nitrogen
Belted drive							
XV	5	350	1050	0.333	2.0	190	Air
XVI	5	450	1050	0.429	2.5	190	Air
XV	5	350	1050	0.333	2.0	190	Air
XVII	5	350	817	0.429	2.5	190	Air
XVIII	5	200	600	0.333	2.0	190	Air

In the belted mode of operation, comparison of Series XV and XVI would show the effect of varying sliding velocity while holding sum velocity constant, while comparison of Series XV and XVII would show the effect of varying sum velocity while holding sliding velocity constant. Here Series XV is common to

both groups of series. Series XVIII was conducted to obtain results at M = 0.333 by using a different combination of V_s and V_t to compare with Series XV.

The detailed results of the various test series are presented in Appendix II. Each table in Appendix II contains the specific break-in and test conditions of each series, the results of each individual test in the series, as well as the average results of the series.

In the following material, the various effects will be examined on the basis of the average results of the appropriate test series. In the examination of the various effects, all parameters of performance such as the failure load, the friction coefficient at failure, the critical temperature, and the minimum lubricant film thickness ratio at failure will be compared. As mentioned previously, from the viewpoint of evaluating the validity of some form of a generalized scuffing criterion, such parameters as the critical temperature, the film thickness ratio, or some other suitable index should be of more fundamental interest. However, the calculation of all these generalized indices involves some assumptions or arbitrary decisions. Currently, the amount of research does not permit an evaluation of the generalized indices to be made with confidence. Therefore, pending additional research, greater emphasis will be given to an examination of the failure load and the friction coefficient at failure. Both parameters are derived from actually measured quantities and are not subject to arbitrary situations other than measurement errors.

2. Comparison of Results for Batch A and B Test Disks

Before beginning the test program with Batch B disks, it was desirable to conduct at least one series of tests under the same conditions used for Batch A disks. This comparison was made for several reasons. (1) the disks, even though made of the same material, were manufactured by two different companies from different heats of steel, (2) Batch B disks were, in general, slightly rougher than Batch A, and (3) the new, more sensitive torquemeters permitted a check on the friction coefficient results previously obtained in testing Batch A disks.

Ten tests were conducted using Batch B disks at T_j = 140°F, V_s = 630 ips, and V_t = 1050 ips. For these tests, the disk tester was operated in the unbelted mode (two shafts independently driven), as was done in all tests with

TABLE II. COMPARISON OF AVERAGE TEST RESULTS FOR BATCH A AND B TEST DISKS WITH LUBRICANT O-67-22, T_j = 140°F, V_s = 630 ips, V_t = 1050 ips

	Before break-in		At end of break-in			At failure									
Batch	δ_1/δ_2, μin.	δ_i, μin.	δ_a, μin.	h_m, μin.	Λ_m	δ_f, μin.	h_{mf}, μin.	Λ_{mf}*	f_f	P_f, lb	w_e, ppi	T_{p2}, °F	T_s, °F	ΔT, °F	T_{cr}, °F
A	8.6/9.3	17.9	14.0	3.5	0.26	19.4	12.3	0.88	0.014	762	6179	169	263	146	409
B	12.0/13.2	25.2	15.1	4.6	0.31	22.3	13.3	0.88	0.022	655	5535	162	231	227	458

*Based on δ_a.

Batch A disks. Table II compares the results with those obtained using Batch A. This table shows the average values of the measured and calculated quantities for 5 tests on the Batch A disks and the 10 tests on Batch B disks. The Batch A results are taken from Table IX of Reference 1. However, they have been modified to correct for the new machine loss and temperature calibrations obtained for lubricant O-67-22. The previously reported values were obtained using the calibration results for lubricant BC, which were the only values available when Reference 1 was published.

As can be seen by comparing these corrected results for Batch A disks with those in Table IX of Reference 1, the main effect of using the new calibration data is to increase the disk surface temperature, T_s. Other quantities remained relatively unaffected by the new calibration results.

In comparing the results of the two batches of disks in Table II, note that the average initial composite surface roughness, δ_i, of Batch B disks is somewhat larger than that of Batch A. However, the break in process brings the

two measured roughnesses to within 1 μin. of each other. At failure, the calculated minimum film thickness differs by only 1 μin. The film thickness ratio at failure, Λ_{mf}, is identical for the two batches. It should be noted that the film thickness ratio at failure should ideally be based on the calculated minimum film thickness and the composite surface roughness at, or immediately prior to, failure. In practice, however, the surface roughness of the disks cannot be measured at, or immediately prior to, failure. Thus the δ_f-measurements must be made after failure. In most cases, the scuffing had progressed all around the disks by the time the machine was stopped, and considerable further damage to the surfaces had occurred. Consequently, no reliable measurement of δ_f can be made. For this reason, this report has based Λ_{mf} on δ_a, the composite surface roughness after break-in, rather than on δ_f.

The friction coefficient is considerably lower for Batch A disks. This difference is attributed mainly to the inaccuracy of the torquemeters that were used in tests with Batch A disks rather than to the difference in surface roughness. From extensive experience with disk testing at SwRI, such a large variation in the friction coefficient at failure with surface roughness has never been observed.

The failure load, P_f, for Batch B disks is 14 percent lower than that for Batch A, and may be attributed to the combination of the effects of a different material batch and disk surface roughness. This difference in P_f is real because P_f is a directly measured quantity. The thermocouple probe temperature, T_{p2}, and the disk surface temperature, T_s, at failure are both higher for Batch A disks due to the higher P_f. For otherwise constant conditions, these two temperatures should be some function of $f_f P_f$. From this consideration, it is seen that the f_f for Batch A disks must be too low. This error in f_f causes the ΔT at failure to be too low for Batch A disks; consequently, the critical temperature, T_{cr}, for Batch A disks must be too low.

3. Effect of Sliding Velocity

The effect of sliding velocity on the failure load is shown in Figure 11. Roman numerals denoting the test series are placed near the data points to aid in identifying the corresponding test conditions shown in Table I. The upper curve in the figure was obtained while operating the tester with the unbelted drive, the lower curve was obtained while operating the tester with the belted drive. For both operating modes, the failure load decreases with increasing V_s. At low values of sliding velocity, the failure load is 2 to 3 times higher when the drive shafts are not belted together. However, this difference in the load-carrying capacity becomes small at high sliding velocities.

This difference in behavior is not fully understood at this time. A possible explanation is that the unbelted shafts permit the disks to shift slightly with respect to each other in the angular sense, even though the speed ratio between shafts is nominally constant. That is, the indicated speed of either shaft will vary by 1 or 2 rpm at typical running speeds of 500 to 3500 rpm. On the other hand, when the shafts are belted together, there is a positive relationship between points on the two disks. Thus, any surface distress that may be initiated when two particular spots come into contact is reinforced as the same two spots continue to come into contact during successive revolutions. It is possible that a small angular shift occurring when the shafts are not belted together is sufficient to prevent two potential trouble spots from coming into contact often enough to cause failure at a lower load. Further work will need to be performed to verify this theory.

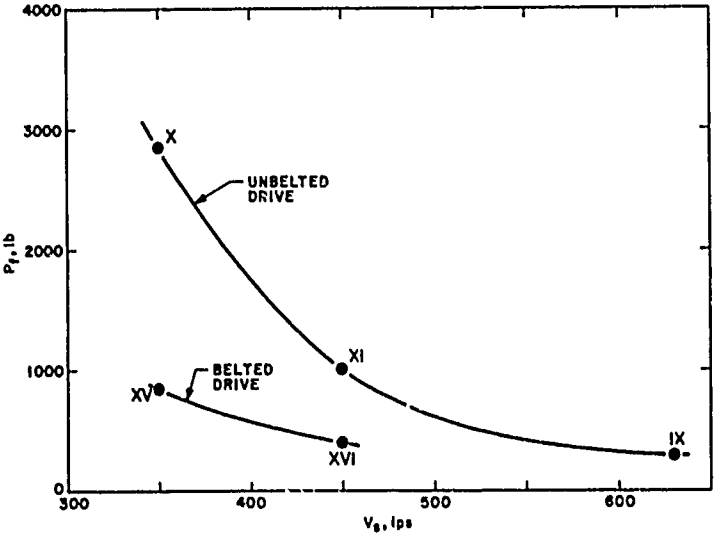

FIGURE 11. EFFECT OF SLIDING VELOCITY ON SCUFFING FAILURE LOAD AT CONSTANT SUM VELOCITY V_t = 1050 ips

A logarithmic presentation of the data in Figure 11 is shown in Figure 12. Note that a nearly linear relationship exists

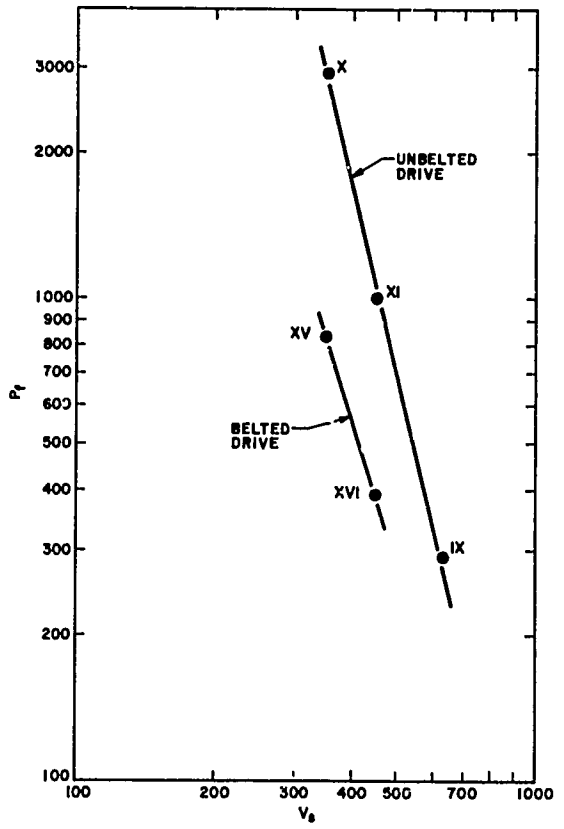

FIGURE 12. LOGARITHMIC PRESENTATION OF DATA FROM FIGURE 11

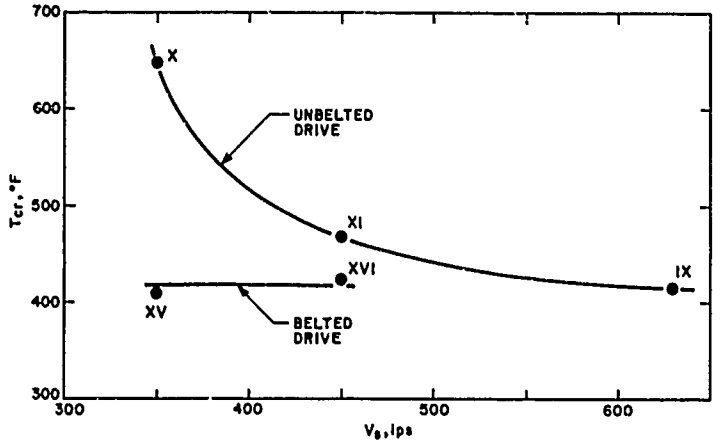

FIGURE 13. EFFECT OF SLIDING VELOCITY ON CRITICAL TEMPERATURE AT CONSTANT SUM VELOCITY V_t = 1050 ips

between log P_f and log V_s, and that the slope for the belted drive results is nearly the same as the slope for the unbelted drive results. Computing the slope of the lines yields

$$P_f \sim \left(\frac{1}{V_s}\right)^{3.88} \tag{9}$$

That is, at constant sum velocity, the scuffing failure load is inversely proportional to sliding velocity raised nearly to the fourth power.

Figure 13 shows the effect of sliding velocity on critical temperature. For the unbelted drive, the critical temperature decreases as the sliding velocity increases; for the belted drive, the critical temperature remains essentially constant. It appears that, at high sliding velocities, the two modes of operation would tend to yield approximately the same critical temperatures.

The effect of sliding velocity on the minimum elastohydrodynamic film thickness ratio at failure is shown in Figure 14. It is seen that, within a range of ±5 percent, this ratio is nearly the same for both modes of drive and nearly constant with respect to sliding velocity.

The effect of sliding velocity on friction coefficient at failure is shown in Figure 15. It is interesting to note that the friction coefficient is not a function of sliding velocity. This is true whether the tester is operated with the belted or the unbelted drive. However, the friction coefficient is higher when the belted drive is used. Whether the higher friction coefficient for the belted drive is due to the repeated interactions between corresponding points on the two disk surfaces, as suggested earlier, remains to be established by further work.

4. Effect of Sum Velocity

The effect of sum velocity on the load at scuffing failure is shown in Figure 16. The effect of increasing V_t while holding V_s constant is to increase the failure load. The failure load is again lower for the belted drive and, as V_t is lowered, the curves tend to merge. A logarithmic presentation of the same data is shown in Figure 17. Unlike the relationship between P_f and V_s, the slopes of these lines are different for the unbelted and belted modes of operation. Computing the slopes of the lines yields for the belted drive

$$P_f \sim (V_t)^{3.66} \tag{10}$$

and for the unbelted drive

$$P_f \sim (V_t)^{1.84} \qquad (11)$$

The effect of sum velocity on critical temperature is shown in Figure 18. The critical temperature increases significantly with increasing sum velocity for the unbelted drive, and increases only slightly for the belted drive. As V_t is decreased, the difference between the two modes of operation becomes less pronounced.

The effect of sum velocity on the minimum elastohydrodynamic film thickness ratio at failure is shown in Figure 19. The belted and unbelted modes give about the same Λ_{mf} to within ±5 percent. However, an increase in sum velocity increases Λ_{mf} moderately.

The behavior of the friction coefficient at failure with sum velocity is shown in Figure 20. It is interesting that while f_f does not vary appreciably with V_s, it does vary with V_t, decreasing with increasing V_t for both the belted and unbelted drives. As was the case when V_t was held constant and V_s varied, the friction coefficient is higher when the belted drive is used.

5. Effect of Sliding to Sum Velocity Ratio

It would be of interest to compare the data at constant sum velocity with the data at constant sliding velocity using some factor common to both test groups. This comparison can be made only by using the ratio of the sliding velocity to the sum velocity.

In Figure 21a, the failure load is shown as a function of velocity ratio, M, for the unbelted drive. It is seen that the results for constant sliding velocity do not differ significantly from those at constant sum velocity; at M = 0.429 and 0.600, the failure load is slightly higher for the constant sliding velocity case. The results for the belted drive are shown in Figure 21b; it is seen that at M = 0.429 the failure load is also slightly

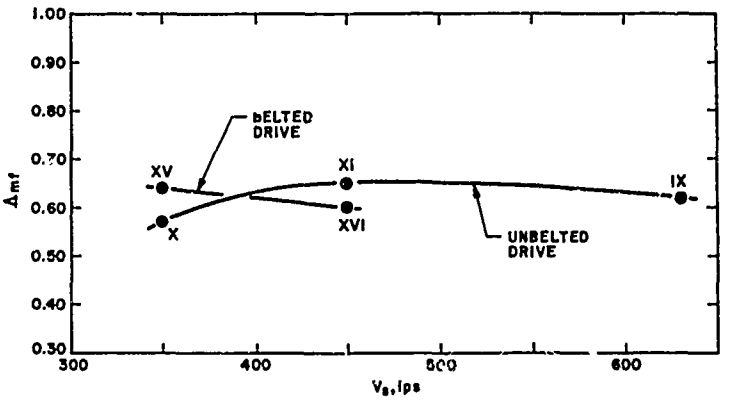

FIGURE 14. EFFECT OF SLIDING VELOCITY ON MINIMUM FILM THICKNESS RATIO AT FAILURE AT CONSTANT SUM VELOCITY V_t = 1050 ips

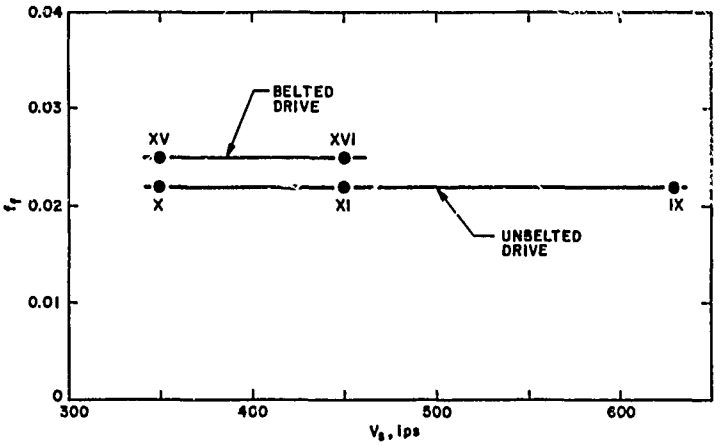

FIGURE 15. EFFECT OF SLIDING VELOCITY ON FRICTION COEFFICIENT AT FAILURE AT CONSTANT SUM VELOCITY V_t = 1050 ips

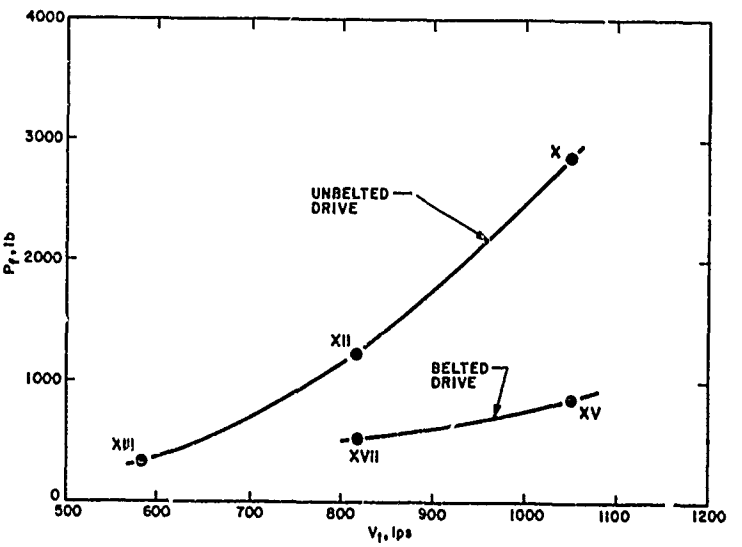

FIGURE 16. EFFECT OF SUM VELOCITY ON SCUFFING FAILURE LOAD AT CONSTANT SLIDING VELOCITY V_s = 350 ips

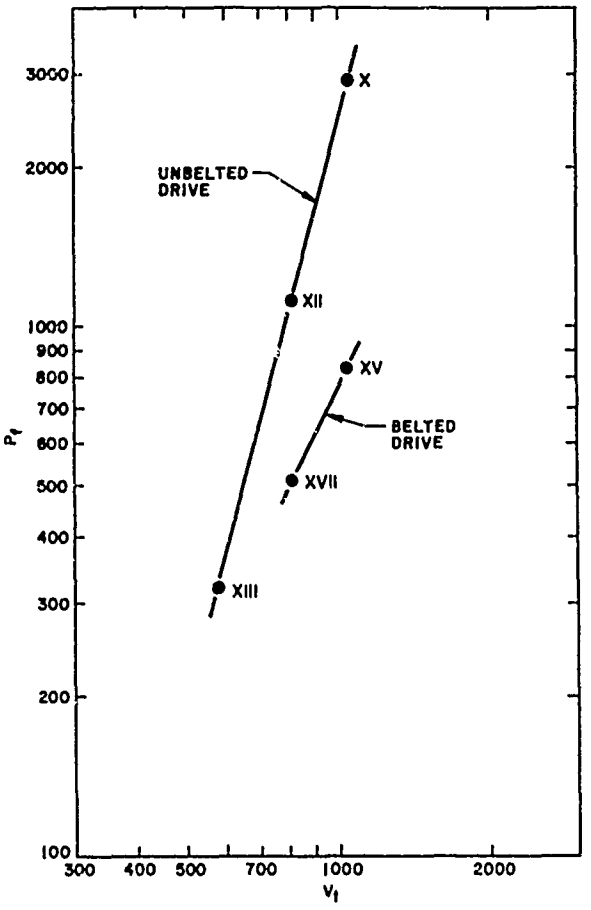

FIGURE 17. LOGARITHMIC PRESENTATION OF DATA FROM FIGURE 16

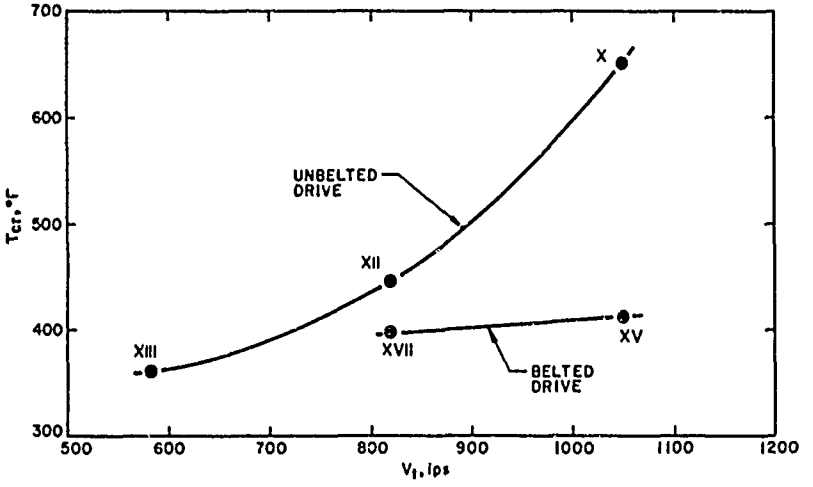

FIGURE 18. EFFECT OF SUM VELOCITY ON CRITICAL TEMPERATURE AT CONSTANT SLIDING VELOCITY V_s = 350 ips

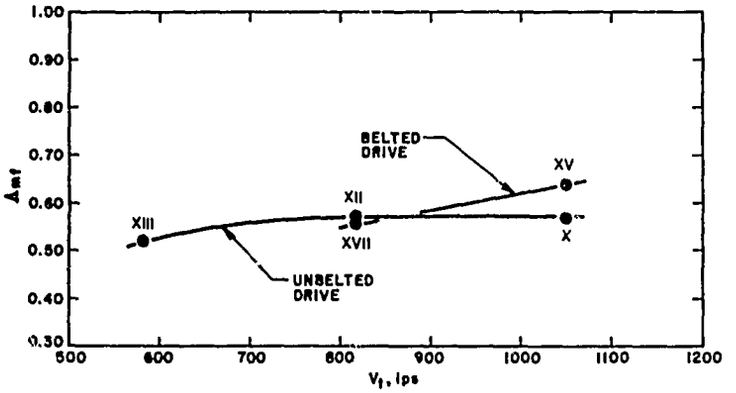

FIGURE 19. EFFECT OF SUM VELOCITY ON MINIMUM FILM THICKNESS RATIO AT FAILURE AT CONSTANT SLIDING VELOCITY V_s = 350 ips

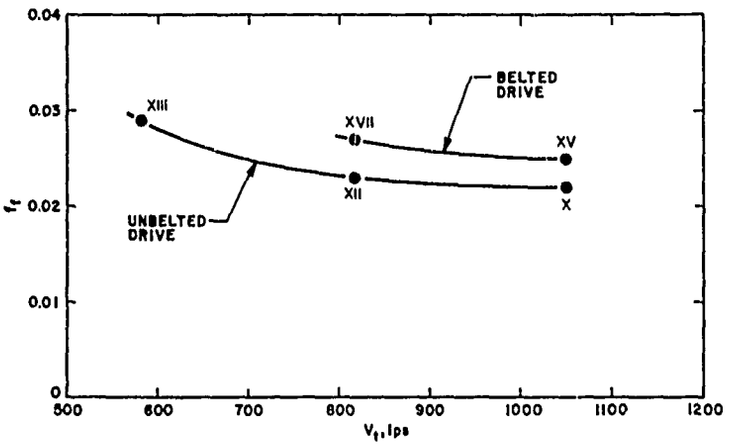

FIGURE 20. EFFECT OF SUM VELOCITY ON FRICTION COEFFICIENT AT FAILURE AT CONSTANT SLIDING VELOCITY V_s = 350 ips

higher for the constant sliding velocity case. For both unbelted and belted drives, the failure load is seen to decrease with increasing M and the decrease is more pronounced with the unbelted drive.

Figure 22a shows the variation of critical temperature with M for the unbelted drive. The critical temperature decreases with increasing M for both the constant sum velocity and constant sliding velocity cases; at M = 0.429 and 0.600, the critical temperature is noticeably higher for the constant sum velocity case. Figure 22b presents the results for the belted drive, and it is seen that for the constant sum velocity case, the critical temperature increases slightly with M, while for the constant sliding velocity case there is a slight decrease. The variation with M is significantly more pronounced for the unbelted drive.

The variation of the minimum EHD film thickness ratio at failure with M for the unbelted drive is shown in Figure 23a. Note that at constant sum velocity, the variation in Λ_{mf} is nonmonotonic, showing first an increase as sliding velocity increases, and then a slight decrease with further increase in sliding velocity. However, at constant sliding velocity, Λ_{mf} is relatively constant. The results are shown for the belted drive in Figure 23b, and it is seen that Λ_{mf} decreases with increasing M for both constant sum velocity and constant sliding velocity tests.

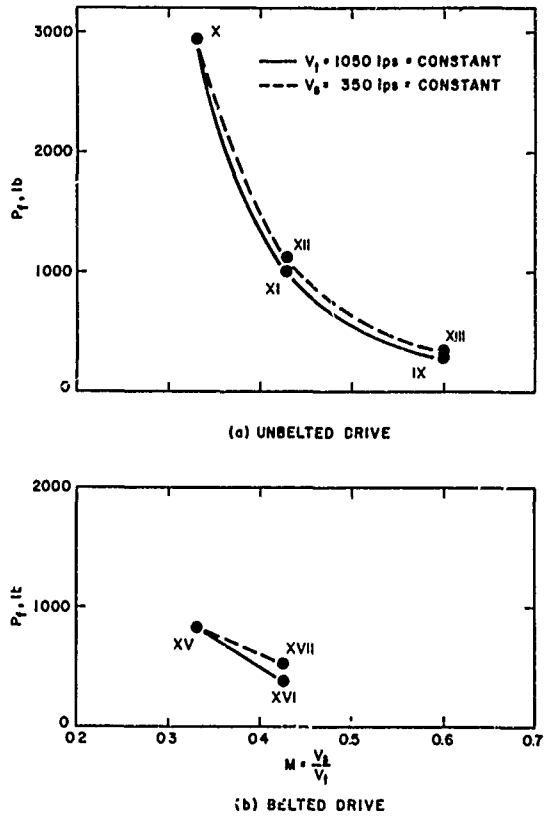

FIGURE 21. EFFECT OF VELOCITY RATIO ON SCUFFING FAILURE LOAD

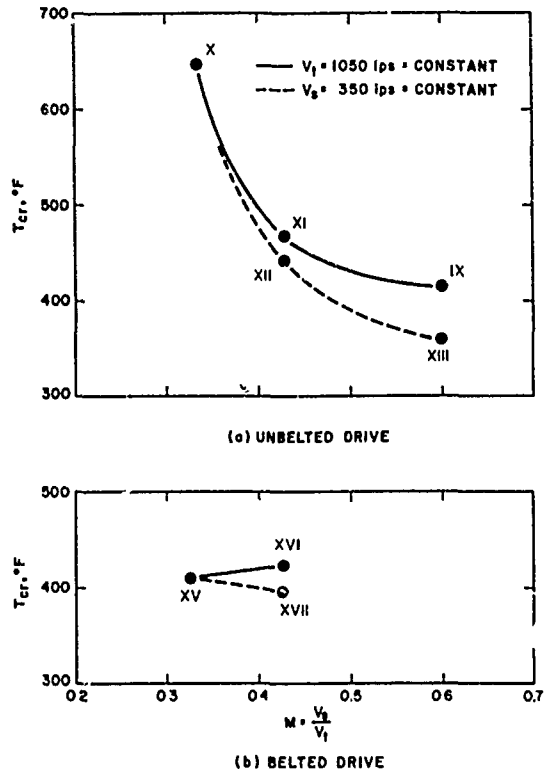

FIGURE 22. EFFECT OF VELOCITY RATIO ON CRITICAL TEMPERATURE

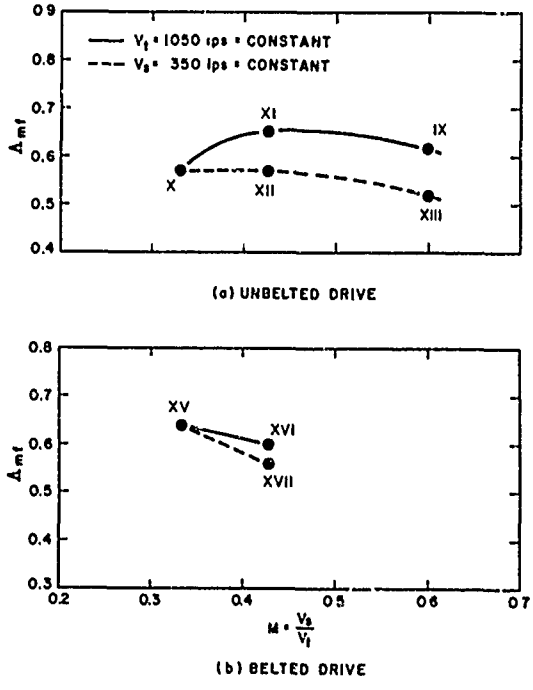

FIGURE 23. EFFECT OF VELOCITY RATIO ON MINIMUM FILM THICKNESS RATIO AT FAILURE

Figure 24a shows the variation of the friction coefficient at failure with the velocity ratio for the unbelted drive. The friction coefficient increases with M at constant sliding velocity; but is constant at constant sum velocity, indicating that the friction coefficient at failure is a function of sum velocity. In Figure 24b the belted drive results exhibit the same trends; that is, f_f increases with M at constant sliding velocity and remains constant at constant sum velocity.

In the practical case of a pair of gears with fixed gear ratio, the velocity ratio, M, is a function only of the local radii of curvature of the meshing teeth and will vary throughout the mesh. The speed of operation of the gear set, however, has no effect on this ratio. Thus, at any particular point along the line of action, a change in the speed of operation will affect the magnitudes of the sliding and sum velocities together; but the ratio will remain constant.

The data from Figures 21 through 24 can be presented in such a manner as to demonstrate this effect of changing the speed of operation of a pair of gears. Figure 25a shows the results for $M = 0.333$, which would be representative of one point along the line of action, and Figure 25b shows the results for $M = 0.429$, which would

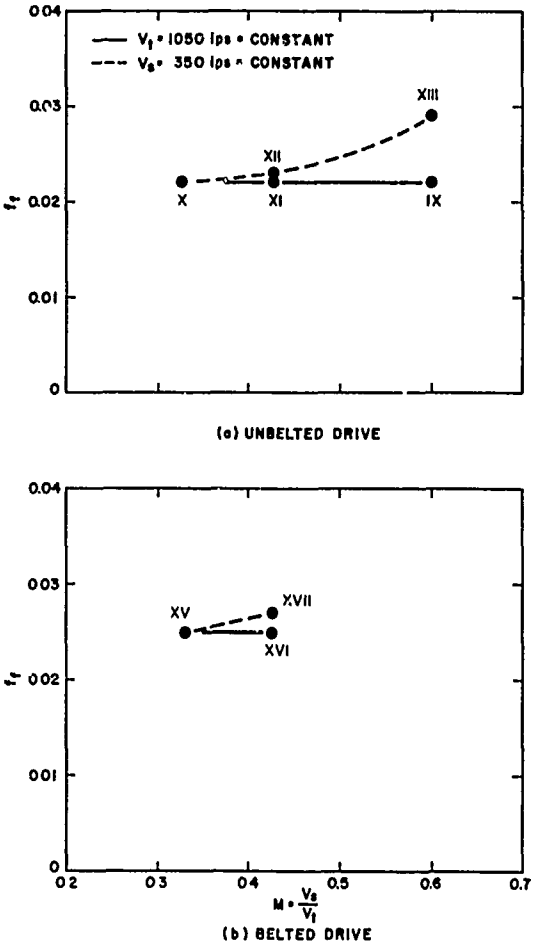

FIGURE 24. EFFECT OF VELOCITY RATIO ON FRICTION COEFFICIENT AT FAILURE

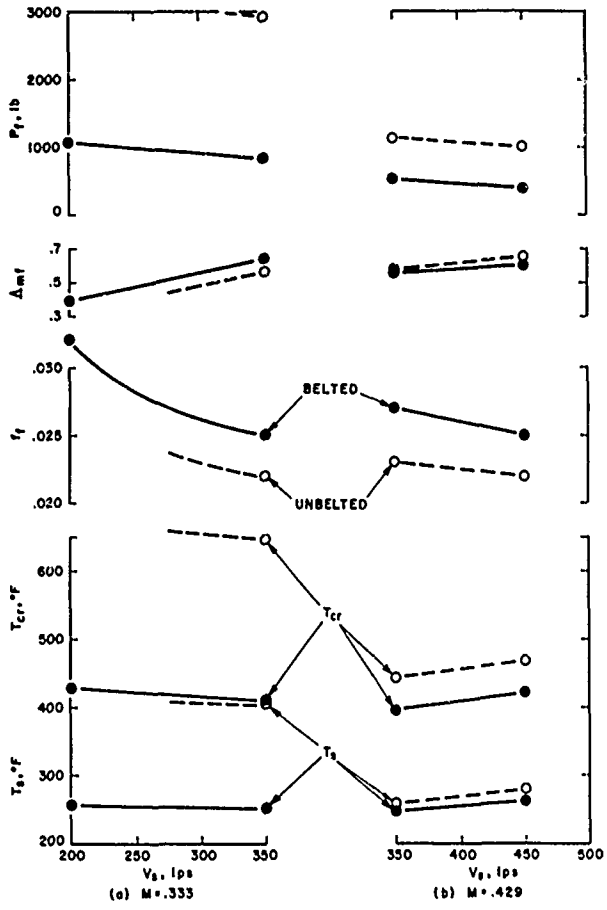

FIGURE 25. EFFECT OF VELOCITY ON SCUFFING PERFORMANCE PARAMETERS AT CONSTANT VELOCITY RATIO

be representative of another point along the line of action. The abscissa is the sliding velocity, V_s, however, the sum velocity, V_t, could have been used just as well since as either one is varied, the other changes such that their ratio remains constant. In addition to the data that were presented earlier, the results of Series XVIII, which were obtained at V_s = 200 ips and V_t = 600 ips with the belted drive, are also shown. At the top of the figure it is seen that the load at failure decreases with increasing speed for both values of M, whether the belted or unbelted drive is used. The minimum film thickness ratio at failure, Λ_{mf}, increases moderately with speed also for both values of M and for both drive modes. The friction coefficient at failure decreases with increasing speed for both values of M and drive modes. However, the critical temperature, T_{cr}, decreases slightly with increasing speed at M = 0.333, but increases with speed at M = 0.429. The same behavior is observed for the surface temperature, T_s, in that it decreases slightly with increasing speed at M = 0.333, but increases with speed at M = 0.429.

6. Effect of Lubricant Jet Temperature

There is a marked effect of lubricant jet temperature on the scuffing failure load, at least for the one set of test conditions investigated. The results are shown in Table III. Series VIII was conducted at T_j = 140°F and Series IX was conducted at the same test conditions except with T_j = 190°F. As seen in the table, the average surface roughness of the disks, both before and after break-in, was about the same for both series. The disks tested at T_j = 140°F failed at a calculated minimum EHD film thickness about 30 percent larger than those tested at T_j = 190°F. This larger film thickness is due to the higher viscosity of the oil at the lower temperature as indicated by the thermocouple probe temperature, T_{p2}. The load at failure in the tests with T_j = 140°F was more than twice

TABLE III. COMPARISON OF AVERAGE TEST RESULTS FOR V_s= 630 ips AND V_t = 1050 ips USING LUBRICANT O-67-22 AT TWO LUBRICANT JET TEMPERATURES

Test series	T_j, °F	Before break-in		At end of break-in			At failure									
		δ_1/δ_2, μin.	δ_i, μin.	δ_a, μin.	h_m, μin.	Λ_m	δ_f, μin.	h_{mf}, μin.	Λ_{mf}*	f_f	P_f, lb	w_e, ppi	T_{p2}, °F	T_s, °F	ΔT, °F	T_{cr}, °F
VIII	140	12.0/13.2	25.2	15.1	4.6	0.31	22.3	13.3	0.88	0.022	655	5535	162	231	227	458
IX	190	12.2/14.0	26.3	16.9	4.5	0.27	22.4	10.4	0.62	0.022	290	3237	197	264	152	415

*Based on δ_a.

that in the tests at T_j= 190°F. The average friction coefficient at failure, f_f, is identical for both series. Since friction coefficient is the same for both series, it is the higher failure load in Series VIII that accounts for the higher critical temperature.

7. Effect of Inert Environment

To determine the effect of an inert environment on scuffing behavior, the disk tester was operated in the presence of nitrogen. The nitrogen used was from a compressed-gas cylinder and contained less than 10 ppm impurities including 5 ppm O_2, 1 ppm H_2, 1 ppm CO_2, 1 ppm CO, with a dew point of −60°F. The nitrogen gas was introduced through the bottom of the lubricant sump beneath the disk enclosure. It was forced to flow up through the lubricant, through the disk enclosure, and out a vent at the top of the enclosure. The lubricant and disk enclosure were purged for 2 hr prior to each test by allowing the nitrogen to flow while the lubricant was circulated through the system at test temperature. The nitrogen continued to flow in this manner throughout the test.

Attempts were made to break in the test disks in the inert environment, using the procedure of permitting the nitrogen to flow through the system with the lubricant circulating at the break-in temperature of 90°F for 2 hr prior to beginning the break-in. However, two sets of disks scuffed during the break in process (one at 1000-lb load and another at the maximum break-in load of 2000 lb). Therefore, this procedure was abandoned and the disks were broken in in an environment of air.

The test results are shown in Table IV. For comparison, the Series XI results, obtained at the same test conditions in an environment of air, are also shown in Table IV. As shown in the table, the average surface roughness of the disks both before and after break-in are the same for both series. In nitrogen, the scuffing failure occurred at a slightly higher calculated minimum EHD film thickness ratio than in air. The friction coefficient at failure was only slightly lower for the tests with nitrogen, while the failure load was significantly lower. The lower load and friction coefficient at failure result in a lower calculated conjunction temperature rise, ΔT. This lower ΔT, combined with the lower surface temperature, T_s, accounts for the large difference in critical temperature.

TABLE IV. COMPARISON OF AVERAGE TEST RESULTS FOR V_s = 450 ips, V_t = 1050 ips, AND T_j = 190°F, USING LUBRICANT O-67-22 IN AIR AND INERT ENVIRONMENTS

Test series	Environment	Before break-in		At end of break-in			At failure									
		δ_1/δ_2, μin.	δ_i, μin.	δ_a, μin.	h_m, μin	Λ_m	δ_f, μin.	h_{mf}, μin	Λ_{mf}*	f_f	P_f, lb	w_e, ppi	T_{p2}, °F	T_s, °F	ΔT, °F	T_{cr}, °F
XI	Air	11.8/10.7	22.4	14.3	5.3	0.37	16.2	9.2	0.65	0.022	1000	7362	199	280	189	469
XIV	Nitrogen	10.6/11.7	22.4	14.2	5.2	0.37	18.3	10.3	0.73	0.020	455	4358	194	225	121	346

*Based on δ_a

These tests indicate that the chemical effects of oxygen and/or moisture in the environment are important in the lubrication process, not only at the higher temperatures and speeds, but also at the lower temperatures and speeds used in the break-in process.

8. Statistical Nature of the Data

The discussion of the results thus far has been concerned with the average test results of the various series of tests rather than the individual test results within each series. It was mentioned previously that with a 10-test series, the failure load varied by a factor of two or three even though all test conditions were the same for each test. This suggests that the scuffing failures may follow a statistical distribution similar to fatigue failures.

Figure 26 shows that the scuffing failure load follows a Weibull distribution relatively well. These are the results from Series X, XI, and IX, where V_t was held constant and V_s was varied. Using these curves, or equations developed from them, one could predict with reasonable accuracy the percentage of a sample of disks that would fail at a given load.

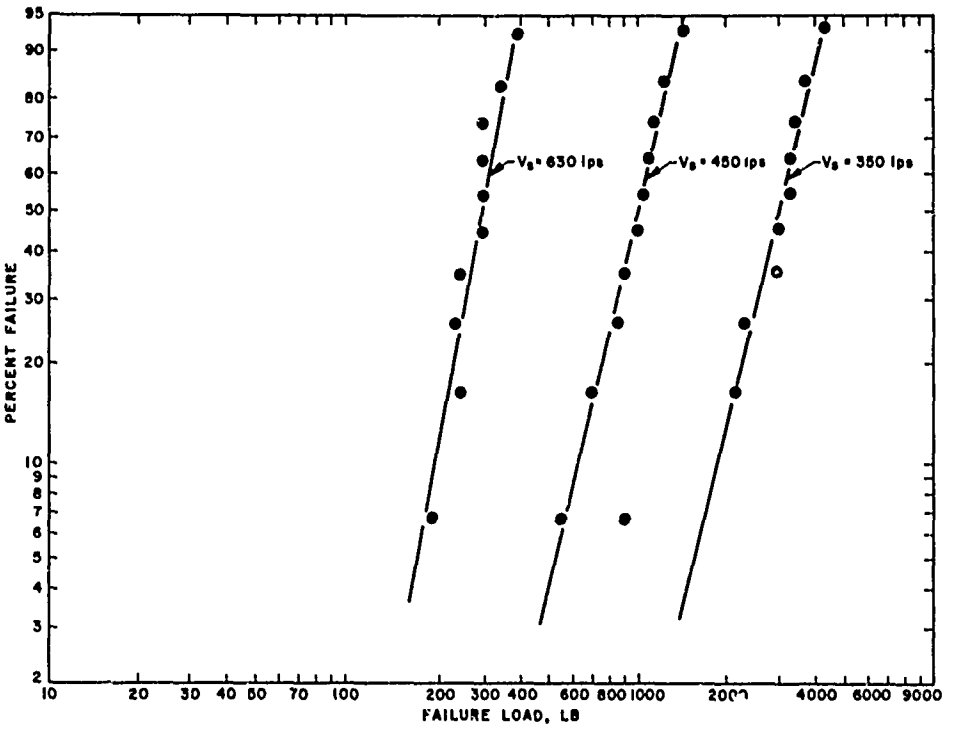

FIGURE 26. WEIBULL PLOT OF SCUFFING FAILURE LOAD AT V_t = 1050 ips

Figure 27 presents the results for Series X, XII, and XIII, where V_s was held constant and V_t was varied. Although the results for the two higher sum velocities follow the Weibull distribution relatively well, the results for V_t = 583 ips do not. This could be indicative of the fact that some phenomenon that affects scuffing at the lower V_t is not present at the two higher values of V_t.

To predict the scuffing failure load over the complete range of operating variables of interest, it would be necessary to have plots similar to those shown in Figures 26 and 27, using either a Weibull or some other distribution function, covering the entire range of the variables. The results of such plots would, at best, be empirical since they do not offer the prospect of generalization. For the purpose of generalization, some suitable generalized scuffing parameter such as the critical temperature, the lubricant film thickness ratio, or some other criterion will have to be treated statistically in a similar manner. Moreover, lubricants, materials,

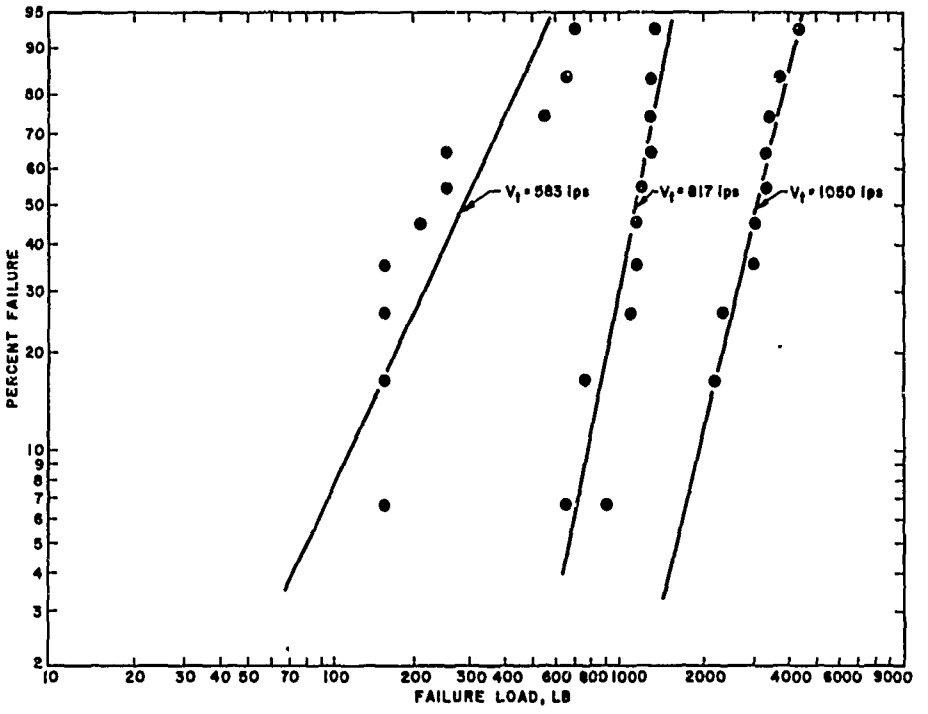

FIGURE 27. WEIBULL PLOT OF SCUFFING FAILURE LOAD AT V_S = 350 ips

and factors other than operating variables alone must also be considered if a generalized scuffing parameter is being sought. Information of such broad scope is not currently available. However, statistical treatment of the data, hitherto not used in gear-scuffing work, is suggested as a possible approach once sufficient data become available.

SECTION V

CONCLUSIONS

From 90 individual scuffing tests conducted using a MIL-L-7808G lubricant (O-67-22) and test disks made from a single heat of AMS 6260 CEVM steel, run at various combinations of sliding and sum velocities, at two lubricant jet temperatures, with two methods of driving the test disks, and in air and nitrogen environments, the following conclusions are drawn:

The load-carrying capacity was found to decrease with increasing sliding velocity, increase with increasing sum velocity, decrease with increasing lubricant jet temperature, decrease with belted as against unbelted drive, and decrease in the presence of an inert environment.

The coefficient of friction at failure was found to change little with increasing sliding velocity, decrease with increasing sum velocity, change little with increasing lubricant jet temperature, increase with belted as against unbelted drive, and decrease in the presence of an inert environment.

The critical temperature was found to decrease with increasing sliding velocity at constant sum velocity, increase with increasing sum velocity at constant sliding velocity, decrease with increasing lubricant jet temperature, decrease with belted as against unbelted drive, and decrease in the presence of an inert environment. At a sliding to sum velocity ratio, M, of 0.333, the critical temperature was found to decrease slightly with increasing speed. However, at $M = 0.429$, the critical temperature was found to increase with increasing speed.

The minimum lubricant film thickness ratio at failure was found to change little with increasing sliding velocity, increase with increasing sum velocity, decrease with increasing lubricant jet temperature, change little with belted as against unbelted drive, and increase in the presence of an inert environment.

Judging from the very low values of the minimum lubricant film thickness ratio experienced at failure, over the entire range of all variables investigated, operation of the disks with lubricant O-67-22, a MIL-L-7808G lubricant, has definitely extended well into the boundary lubrication regime before scuffing failure. This confirms the earlier findings in Reference 1, in which it was noted that a straight mineral oil failed as soon as the operation moved from elastohydrodynamic into a boundary lubrication regime. Two synthetic oils, however, including lubricant O-67-22, were able to operate substantially into the boundary lubrication regime without failure. This being the case, the applicability of the lubricant film thickness ratio as a generalized scuffing criterion, will require more convincing theoretical and practical justification.

The critical temperature, the more popular generalized scuffing criterion, has been found to behave differently for the belted and unbelted drives. With the unbelted drive, the critical temperature is clearly far from being constant with respect to any of the variables investigated herein. On the other hand, the critical temperature remained fairly constant with the belted drive, for which it was only possible to study the effects of sliding and sum velocities over a rather limited range. The nonconstancy of the critical temperature for the unbelted drive with respect to all operating variables, its contrasting behaviors with respect to the method of drive, and especially its lack of consistent behavior with respect to speed at two different sliding to sum velocity ratios, cannot be explained by any conventional theoretical justification of the critical temperature hypothesis. Even as a strictly arbitrary scuffing criteria, its generalized relationship with all operating variables has yet to be developed. This relationship cannot be accomplished with confidence without a great deal of additional research.

APPENDIX I

DETERMINATION OF CONSTANTS IN EQ. (6)

Since, by definition, the disk friction torque, T_f, as measured by the two torquemeters must be equal, Eq. (2) may be subtracted from Eq. (1) to give

$$T_{r1} - T_{r2} = T_{m1} + T_{m2} \tag{12}$$

From Eq. (5), for the upper shaft

$$T_{m1} = aP + bN_1\mu_f^c \tag{13}$$

and for the lower shaft

$$T_{m2} = aP + bN_2\mu_f^c \tag{14}$$

where

T_{m1} – machine-loss torque for upper shaft, in.-lb

T_{m2} – machine-loss torque for lower shaft, in.-lb

N_1 – upper shaft speed, rpm

N_2 – lower shaft speed, rpm

and other symbols were defined after Eq. (5). Now substituting Eqs. (13) and (14) into Eq. (12)

$$T_{r1} - T_{r2} = 2aP + bu_f^c(N_1 + N_2) \tag{15}$$

But N_1 can be related to N_2 by the ratio of the shaft rotational speeds, $S = N_1/N_2$, so that Eq. (15) becomes

$$T_{r1} - T_{r2} = 2aP + (S + 1)bN_2\mu_f^c \tag{16}$$

To determine the constant a, let S, N_2, and μ_f be held constant and the load be varied between two values, say P and P'. Then for load P, Eq. (16) gives

$$(T_{r1} - T_{r2}) = 2aP + (S + 1)bN_2\mu_f^c \tag{17}$$

or rearranging

$$(S + 1)bN_2\mu_f^c = (T_{r1} - T_{r2}) - 2aP \tag{18}$$

where $(T_{r1} \quad T_{r2})$ is the difference in torquemeter readings corresponding to load P. For load P', Eq. (16) gives

$$(T_{r1} - T_{r2})' = 2aP' + (S + 1)bN_2\mu_f^c \tag{19}$$

or rearranging

$$(S + 1)bN_2\mu_f^c = (T_{r1} - T_{r2})' - 2aP' \tag{20}$$

where $(T_{r1} \quad T_{r2})'$ is the difference in torquemeter readings corresponding to load P'. Equating Eqs. (18) and (20), and solving for the constant a, one obtains:

$$a = \frac{(T_{r1} - T_{r2})' - (T_{r1} - T_{r2})}{2(P' - P)} \tag{21}$$

To determine the constant c, the data from two runs are needed where P and N_2 are the same, but the lubricant viscosity is varied from μ_j to μ_j'. Then for viscosity μ_j, Eq. (16) gives

$$(T_{r1} - T_{r2}) = 2aP + (S + 1)bN_2\mu_j^c \tag{22}$$

or rearranging

$$(S + 1)bN_2 = \frac{(T_{r1} - T_{r2}) - 2aP}{\mu_j^c} \tag{23}$$

where $(T_{r1} - T_{r2})$ is the difference in torquemeter readings corresponding to the case where viscosity is μ_j. For viscosity μ_j', Eq. (16) gives

$$(T_{r1} - T_{r2})' = 2aP + (S + 1)bN_2\mu_j'^c \tag{24}$$

or rearranging

$$(S + 1)bN_2 = \frac{(T_{r1} - T_{r2})' - 2aP}{\mu_j'^c} \tag{25}$$

where $(T_{r1} - T_{r2})'$ is the difference in torquemeter readings corresponding to the case where viscosity is μ_j'. Equating Eqs. (23) and (25) and rearranging

$$\left(\frac{\mu_j}{\mu_j'}\right)^c = \frac{(T_{r1} - T_{r2}) - 2aP}{(T_{r1} - T_{r2})' - 2aP} \tag{26}$$

Taking the logarithm of both sides

$$c\,\ell n\left(\frac{\mu_j}{\mu_j'}\right) = \ell n\left[\frac{(T_{r1} - T_{r2}) - 2aP}{(T_{r1} - T_{r2})' - 2aP}\right] \tag{27}$$

or

$$c = \frac{\ell n\left[\dfrac{(T_{r1} - T_{r2}) - 2aP}{(T_{r1} - T_{r2})' - 2aP}\right]}{\ell n\ \dfrac{\mu_j}{\mu_j'}} \tag{28}$$

To determine the constant b, Eq. (16) may be written

$$b = \frac{(T_{r1} - T_{r2}) - 2aP}{(S + 1)N_2\mu_j^c} \tag{29}$$

from which b may be calculated since all other quantities are now known.

APPENDIX II

SUMMARIES OF TEST RESULTS

The results of all tests performed during this reporting period are summarized in this appendix. Each table contains the individual results of a series of replicate tests conducted under one set of conditions, as well as the average results of the series. Summaries of the results of Series I through VII, conducted with lubricants B, 0-64-2, and 0-67-22, together with Batch A of AMS 6260 steel test disks, were presented in a previous report.[1] This appendix presents only the results of Series VIII through XVIII, conducted with lubricant 0-67-22 in combination with Batch B of AMS 6260 steel test disks.

The break-in and test conditions, as well as other pertinent details about each series, are shown at the top of each table. Unless otherwise specified, the series was conducted in an air environment and with the unbelted drive system.

Break-In Conditions. As is customary, the break-in process involves operating the test disks through a step-load sequence, at a sufficiently low lubricant jet temperature and at sufficiently low sliding and sum velocities, in such a manner that, while no scuffing should occur during the break-in, the final or maximum break-in load should be higher than the anticipated scuffing failure load to be obtained later during the test. The rationale behind this procedure is that if the failure load obtained during test should be higher than the maximum break-in load, then the failure could occur at the edge, i.e., on the outside, of the broken-in track so that this failure load could be lower than it would have been had it occurred inside of the broken in track. We have followed this break-in procedure throughout this program, but have found that edge failures still occasionally occur. These edge failures are believed to be caused by the shape of the constriction in the conjunction due to the effect of side flow in the conjunction.

As shown at the top of the tables, all break-ins were conducted at the same lubricant jet temperature of 90°F. However, the break-in speed conditions and the load schedule were not strictly the same for all series. In the interest of brevity, the break-in load schedule is shown in an abbreviated form. For example, the notation 4 X 300(15) indicates four load steps of 300-lb increments, each step being run for 15 min.

For Series VIII and IX, the break-in conditions were identical. The maximum break-in load of 1200 lb exceeded all observed failure loads. When Series X was begun, the same load schedule and speed conditions were used for Test B24. In this test, failure occurred at 900 lb, which is less than the maximum break-in load of 1200 lb. For the next two tests, B25 and B26, the failure load exceeded this maximum break-in load. It appeared from the observed failure loads that a 3000-lb maximum break-in load might be more appropriate. This 3000-lb load was implemented for Test B27, however, the shaft speeds had to be increased to prevent the disks from chattering at the high loads. In the next attempt at break in (Test B28, which was discarded), the disks scuffed at the 3000-lb load, even with the increased shaft speeds. It was then decided to reduce the maximum break-in load to 2000 lb, but to continue using the higher shaft speeds. From Test B29 on, the break-in was standardized with V'_s = 47 ips, V'_t = 141 ips, with a maximum break-in load of 2000 lb achieved in four increments of 500 lb, each run for 15 min. No difficulties were encountered with break-in thereafter.

Test Conditions. The test conditions were varied for each series as noted at the top of each table. However, the test load schedule, designated as 50(3) herein, was the same throughout the tests. After the speed conditions were reached, increments of 50 lb of load were applied, allowing 3 min at each load step to achieve equilibrium, until scuffing failure was detected by the operator. The "Mode" column in the tables shows the mode or indication of failure (CR for contact resistance, T for torque increase). Each failure was verified by visual inspection after stopping the test.

Other Symbols. As for the various quantities tabulated, most have already been discussed, and all are defined in the List of Symbols. The metal monitor reading (mm) is shown before break-in (BBI), after break-in (ABI), and after test (AT). The first value is for the upper disk and the second is for the lower disk. The metal monitor reading itself does not yield any quantitative information about the character of the disk surface, but a change in metal

monitor reading may suggest a change in the surface qualities of the disks.[1] For example, the formation of a surface film due to chemical reaction between the lubricant and metal surface can generally be detected by a change in the metal monitor reading.

The tables also show the composite surface roughness of the pair of disks before break-in (δ_i), after break-in (δ_a), and after failure (δ_f), as well as the film thickness ratios at the end of break-in (Λ_m) and at failure (Λ_{mf}). Details of calculations are given in Reference 1. It should be pointed out that the film thickness ratio at failure, as used in this report, has been calculated using the composite surface roughness after break-in. This quantity should preferably be based on the composite surface roughness just before, rather than after, failure since it is intended to indicate the degree of asperity interaction occurring just before failure. Moreover, in most cases, the scuffing failure extends completely around the periphery of the disks so that δ_f is usually higher than δ_a and cannot, in general, be accurately measured. Therefore, rather than using the questionable δ_f, the tabulated Λ_{mf} has been calculated using δ_a in all cases.

TABLE V. SUMMARY OF RESULTS FOR SERIES VIII

Test lubricant: O-67-22
Test disks: AMS 6260 (Batch B)
Break-in conditions: T_j = 90°F, V_s = 24 ips, V_t = 70 ips, 4 × 300(15)
Test conditions: T_j = 140°F, V_s = 630 ips, V_t = 1050 ips, 50(3)

Test no	mm			Before break-in		At end of break-in			At failure										
	BBI	ABI	AT	δ_1/δ_2, μin.	δ_3, μin.	δ_a, μin.	h_m, μin	Λ_m	δ_f, μin.	h_m, μin	Λ_{mf}*	f_f	P_f, lb	w_e, ppi	T_{p2}, °F	T_s, °F	ΔT, °F	T_{cr}, °F	Mode
B3	1.0/0.5	3.0/2.2	2.0/1.2	11.7/14.5	26.2	14.4	4.6	0.32	21.4	13.2	0.92	0.022	450	4355	164	243	190	433	CR
B4	2.0/1.0	3.0/3.0	2.5/2.5	12.6/16.3	28.9	15.2	4.6	0.30	21.4	13.5	0.89	0.021	450	4355	162	234	183	417	CR
B5	1.0/1.2	3.2/3.0	1.5/2.0	13.1/12.3	25.4	14.7	4.6	0.31	23.4	9.8	0.67	0.022	1000	7416	191	357	287	644	CR
B6	0.0/1.6	2.0/3.2	1.2/2.2	11.7/12.9	24.6	13.6	4.6	0.34	20.2	11.7	0.86	0.022	950	7167	171	271	288	559	CR,I
B7	1.5/2.5	3.0/3.3	1.5/2.6	14.3/15.1	29.4	14.9	4.5	0.30	20.4	14.4	0.97	0.024	500	4672	154	200	225	425	CR,I
B9	2.5/0.5	3.0/2.0	1.5/0.0	11.2/16.2	27.4	15.5	4.8	0.31	22.7	14.0	0.91	0.021	650	5565	155	203	220	423	CR,I
B10	2.3/1.6	3.2/2.8	1.5/1.0	10.6/12.4	23.0	15.8	4.7	0.30	22.0	14.0	0.89	0.018	650	5565	155	203	191	394	CR,I
B11	2.7/3.2	3.0/3.0	2.0/1.6	9.9/10.3	20.2	15.0	4.6	0.31	20.3	12.6	0.84	0.024	900	6913	163	237	290	527	CR,I
B12	3.3/2.0	3.4/2.2	1.0/2.5	13.0/13.4	26.4	15.8	4.6	0.29	25.3	14.7	0.93	0.022	500	4672	152	191	207	398	CR,I
B13	2.0/2.5	2.5/2.5	2.5/1.0	12.2/16.6	20.8	16.1	4.6	0.29	25.5	15.3	0.95	0.020	500	4672	148	174	189	363	CR,I
			Average	12.0/13.2	25.2	15.1	4.6	0.31	22.3	13.3	0.88	0.022	655	5535	162	231	227	458	
			Std dev	1.3/2.5	3.1	0.8	0.1	0.01	2.0	1.6	0.08	0.000	217	1207	12	53	44	89	

*Based on δ_4

TABLE VI. SUMMARY OF RESULTS FOR SERIES IX

Test lubricant: O-67-22
Test disks: AMS 6260 (Batch B)
Break-in conditions: T_j = 90°F, V_s = 24 ips, V_t = 70 ips, 4 × 300(15)
Test conditions: T_j = 190°F, V_s = 630 ips, V_t = 1050 ips, 50(3)

Test no	mm			Before break-in		At end of break-in			At failure										
	BBI	ABI	AT	δ_1/δ_2 μin.	δ_3, μin.	δ_a, μin	h_m, μin.	Λ_m	δ_f, μin	h_m, μin	Λ_{mf}*	f_f	P_f, lb	w_e, ppi	T_{p2}, °F	T_s, °F	ΔT, °F	T_{cr}, °F	Mode
B14	1.2/1.0	1.8/2.0	1.0/0.5	9.4/12.8	22.2	16.1	4.6	0.29	23.4	10.0	0.62	0.022	400	4026	199	276	182	458	CR,I
B15	0.5/2.0	1.2/3.0	0.5/2.5	11.3/14.1	25.4	17.6	4.5	0.26	22..	10.5	0.60	0.025	250	2943	197	260	162	422	CR,I
B16	2.5/2.0	2.2/2.0	1.3/1.6	10.7/12.4	23.1	16.8	4.5	0.27	22.5	10.3	0.61	0.021	300	3323	197	263	148	411	CR,I
B17	1.0/0.6	1.0/1.5	1.2/2.0	12.2/14.6	26.8	17.2	4.5	0.26	24.0	10.3	0.60	0.022	300	3323	198	270	159	429	CR,I
B18	1.0/0.0	1.0/0.0	1.8/0.0	11.6/12.9	29.5	19.1	4.6	0.24	21.7	10.5	0.55	0.020	250	2943	197	256	130	386	CR,I
B19	0.5/2.5	0.5/2.5	0.5/2.0	12.8/17.0	25.8	16.6	4.6	0.28	20.9	10.3	0.62	0.022	300	3323	198	270	156	426	CR,I
B20	1.5/2.5	1.4/2.6	1.5/2.6	13.1/16.2	29.3	17.0	4.5	0.26	22.3	10.1	0.60	0.020	350	3683	198	270	150	420	CR,I
B21	1.5/1.5	1.8/1.5	2.2/2.0	12.9/16.5	29.4	18.9	4.5	0.24	24.3	10.5	0.56	0.020	250	2943	197	260	127	387	CR,I
B22	2.0/1.0	1.5/0.8	2.0/1.0	12.5/15.3	27.8	15.4	4.5	0.29	22.0	10.3	0.67	0.022	300	3323	197	260	153	413	CR,I
B23	1.0/1.5	2.0/2.5	0.5/1.2	15.9/12.3	28.2	14.5	4.6	0.32	21.0	10.8	0.74	0.025	200	2536	196	253	149	402	CR,I
			Average	12.2/14.0	26.3	16.9	4.5	0.27	22.4	10.4	0.62	0.022	290	3237	197	264	152	415	
			Std dev	1.7/1.6	2.5	1.4	0.1	0.02	1.2	0.2	0.05	0.003	57	422	1	7	16	21	

*Based on δ_4

TABLE VII. SUMMARY OF RESULTS FOR SERIES X

Test lubricant: O-67-22
Test disks: AMS 6260 (Batch B)
Break-in conditions: T_j = 90°F, V_s = 47 ips, V_t = 141 ips, 4 × 500(15)
Test conditions: T_j = 190°F, V_s = 350 ips, V_t = 1050 ips, 50(3)

Test no.	mm			Before break-in		At end of break-in			At failure										
	BBI	ABI	AT	δ_s/δ_t, μin	δ_t, μin	δ_s, μin	h_m, μin	Λ_m	δ_f, μin	h_m, μin	Λ_{mf}*	t_f	P_f, lb	w_e, ppi	T_{p2}, °F	T_s, °F	ΔT_s, °F	T_{cr}, °F	Mode
B24	0.0/1.3	−1.0/−2.0	−2.0/−0.5	16.1/17.6	33.7	16.6	4.6	0.28	38.3	9.3	0.56	0.030	900	6,913	198	270	194	464	CR,I
B25	1.3/1.5	0.4/1.0	2.0/1.6	10.4/11.7	22.1	14.4	4.6	0.32	17.7	7.8	0.54	0.022	2,950	15,254	208	370	255	625	CR,T
B26	0.5/1.5	−0.2/0.5	1.0/0.5	11.7/10.1	21.8	15.8	4.5	0.28	16.8	7.6	0.48	0.022	3,300	16,438	210	390	271	661	CR,T
B27	0.0/1.0	−0.5/0.8	0.0/0.2	14.6/11.4	26.0	13.2	4.2	0.32	19.1	6.8	0.51	0.023	2,300	12,922	231	603	238	841	CR,T
B29	0.5/0.2	1.0/0.5	1.5/1.6	11.5/12.2	27.7	12.3	5.4	0.44	15.1	8.1	0.66	0.023	2,150	12,354	206	353	226	579	CR,T
B30	0.0/1.3	−0.5/0.2	1.5/1.6	10.0/10.5	20.5	13.1	5.2	0.40	14.2	7.5	0.57	0.019	3,450	16,932	217	400	247	653	CR,T
B31	1.5/1.5	1.2/2.5	2.5/2.5	10.0/12.6	22.6	11.5	5.2	0.45	13.9	7.1	0.62	0.018	4,350	19,762	216	453	2..	705	CR
B32	0.0/1.0	0.8/2.0	2.0/1.0	11.2/13.1	24.3	13.3	5.2	0.39	16.1	7.5	0.56	0.020	3,300	16,438	213	420	253	673	CR,T
B33	1.5/1.5	2.0/3.2	2.0/1.5	11.0/11.1	22.1	12.6	5.2	0.41	16.7	7.7	0.61	0.022	3,000	15,426	209	380	254	634	CR,I
B34	1.6/2.5	3.0/3.2	2.2/2.0	11.8/14.1	25.9	13.6	5.2	0.38	14.0	7.3	0.54	0.020	>3,700	17,741	215	436	262	>698	None†
			Average	11.8/12.3	24.5	13.6	4.9	0.36	16.7	7.7	0.57	0.022	2,940	14,715	212	405	243	648	
			Std. dev.	2.1/2.2	4.1	1.7	0.4	0.07	7.6	0.7	0.06	0.003	959	3,653	9	90	22	190	

*Based on δ_s
†Support bearing failed. Test terminated before scuffing occurred. Average and standard deviation do not include this test

TABLE VIII. SUMMARY OF RESULTS FOR SERIES XI

Test lubricant: O-67-22
Test disks: AMS 6260 (Batch B)
Break-in conditions: T_j = 90°F, V_s = 47 ips, V_t = 141 ips, 4 × 500(15)
Test conditions: T_j = 190°F, V_s = 450 ips, V_t = 1050 ips, 50(3)

Test no	mm			Before break-in		At end of break-in			At failure										
	BBI	ABI	AT	δ_s/δ_t, μin	δ_t, μin	δ_s, μin	h_m, μin	Λ_m	δ_f, μin	h_m, μin	Λ_{mf}*	t_f	P_f, lb	w_e, ppi	T_{p2}, °F	T_s, °F	ΔT_s, °F	T_{cr}, °F	Mode
B35	0.0/1.0	0.0/1.5	0.5/1.0	16.7/13.6	30.3	16.9	5.2	0.31	19.5	10.0	0.59	0.026	550	4978	194	230	137	362	CR,I
B37	2.5/1.0	2.2/2.0	2.5/1.0	8.6/10.5	19.1	15.1	5.2	0.34	15.3	9.2	0.61	0.021	1100	[illegible]3	198	270	193	463	CR,I
B38	1.2/1.0	2.0/1.6	1.5/1.2	10.5/9.9	20.4	15.6	5.1	0.33	14.9	9.3	0.64	0.021	1000	[illegible]416	197	260	190	450	CR,I
B39	1.0/1.2	1.6/1.5	1.2/1.5	9.3/10.5	20.3	13.7	5.2	0.38	14.7	8.6	0.63	0.022	1450	9501	203	320	238	558	CR,I
B40	−1.0/0.5	0.5/2.0	0.6/1.5	14.6/11.7	26.3	14.8	5.5	0.37	18.1	9.5	0.64	0.022	700	5547	198	270	165	435	CR,I
B41	0.5/1.2	2.0/1.0	2.0/1.2	13.6/11.1	24.7	16.0	5.2	0.33	17.6	9.2	0.57	0.023	900	6913	200	290	189	479	CR,I
B42	1.5/0.5	1.5/0.0	1.6/0.5	11.7/10.1	21.8	14.0	5.2	0.37	16.9	9.5	0.68	0.022	850	6655	196	253	178	431	CR,I
B43	1.2/1.0	0.6/1.2	1.0/1.8	13.2/7.7	20.9	12.6	5.1	0.40	14.2	8.8	0.70	0.023	1250	8606	202	310	228	538	CR,I
B44	1.9/0.9	0.5/0.0	1.5/1.0	9.0/9.9	18.9	11.7	5.3	0.45	14.2	8.9	0.76	0.020	1150	8140	202	310	190	500	CR,I
B45	2.0/1.7	0.6/1.0	1.9/2.0	9.8/11.6	21.4	14.0	5.6	0.40	16.4	9.1	0.65	0.021	1050	7661	200	290	188	478	CR,I
			Average	11.8/10.7	22.4	14.5	5.3	0.37	16.2	9.2	0.65	0.022	1000	7362	199	280	184	469	
			Std dev	2.7/1.5	3.6	1.5	0.2	0.04	1.8	0.4	0.06	0.001	263	1325	3	23	30	56	

*Based on δ_s

TABLE IX. SUMMARY OF RESULTS FOR SERIES XII

Test lubricant: O-67-22
Test disks: AMS 6260 (Batch B)
Break-in conditions: T_j = 90°F, V_s = 47 ips, V_t = 141 ips, 4 × 500(15)
Test conditions: T_j = 190°F, V_s = 350 ips, V_t = 817 ips, 50(3)

Test no	mm			Before break-in		At end of break-in			At failure										
	BBI	ABI	AT	h_a, h_s, μin	δ_t μin	δ_a, μin	h_m, μin	λ_m	h_f, μin	h_m, μin	λ_{mf}*	f_f	P_f, lb	w_e, ppi	T_{p2}, °F	T_s, °F	ΔT_s, °F	T_{cr}, °F	Mode
B46	1.2/0.5	0.5/0.5	1.2/0.8	8.4/9.7	18.1	10.6	5.3	0.50	11.6	7.5	0.71	0.022	1350	9059	198	273	203	476	T
B47	1.2/0.5	2.0/1.6	1.8/1.6	10.4/12.8	23.2	13.4	5.2	0.39	15.5	7.5	0.56	0.022	1300	8833	199	276	195	471	CR,I
B48	1.0/3.5	2.0/2.0	1.8/2.2	14.1/16.4	17.5	14.1	5.4	0.38	15.0	7.7	0.55	0.024	1100	7903	197	260	193	453	CR,I
B49	1.0/2.5	1.2/2.0	1.2/2.0	9.1/11.5	20.6	14.5	5.3	0.37	15.3	8.2	0.57	0.023	750	6122	194	230	156	386	CR,I
B50	1.0/2.0	2.4/2.4	2.2/2.5	9.7/8.7	18.4	12.3	5.1	0.41	16.0	7.7	0.62	0.021	1300	8833	197	256	190	446	CR,I
B51	1.2/1.0	2.4/2.0	2.5/2.0	8.6/12.3	20.9	14.0	5.1	0.36	16.2	8.3	0.59	0.026	650	5565	195	236	163	399	CR,I
B53	1.6/1.6	2.4/1.5	2.2/1.5	12.0/10.7	22.7	16.9	5.5	0.33	16.7	7.7	0.46	0.025	1150	8140	197	260	208	468	CR,I
B54	1.0/1.0	1.5/1.0	1.5/1.5	9.2/12.8	22.0	15.9	5.5	0.35	15.2	7.6	0.48	0.024	1200	8374	198	270	208	478	CR,I
B55	2.8/0.5	3.2/2.0	2.2/0.8	7.1/10.3	17.4	12.4	6.0	0.48	15.9	7.6	0.61	0.019	1300	8833	198	270	174	444	CR,I
B56	1.0/1.5	1.8/2.2	1.2/1.0	12.1/12.1	24.2	13.8	5.5	0.40	18.4	7.8	0.56	0.020	1150	8140	196	253	167	420	CR,I
			Average	9.8/10.7	20.5	13.8	5.4	0.40	15.6	7.8	0.57	0.023	1125	7980	197	258	186	444	
			Std dev	1.6/2.0	2.5	1.8	0.3	0.06	1.7	0.3	0.07	0.002	240	1195	4	15	19	37	

*Based on δ_a

TABLE X. SUMMARY OF RESULTS FOR SERIES XIII

Test lubricant: O-67-22
Test disks: AMS 6260 (Batch B)
Break-in conditions: T_j = 90°F, V_s = 47 ips, V_t = 141 ips, 4 × 500(15)
Test conditions: T_j = 190°F, V_s = 350 ips, V_t = 583 ips, 50(3)

Test no	mm			Before break-in		At end of break-in			At failure										
	BBI	ABI	AT	h_a, μin	δ_t μin	δ_a μin	h_m, μin	λ_m	h_f μin	h_m, μin	λ_{mf}*	f_f	P_f lb	w_e ppi	T_{p2} °F	T_s °F	ΔT °F	T_{cr} °F	Mode
B58	1.0/2.0	2.0/1.6	1.6/2.0	12.1/8.9	21.0	11.7	5.2	0.44	18.3	7.7	0.66	0.023	150	2094	193	193	85	280	CR,I
B59	1.2/1.5	1.0/1.0	1.2/2.0	8.1/10.2	18.3	12.1	5.3	0.44	17.0	7.2	0.59	0.023	250	2943	193	220	112	332	CR,I
B60	0.8/1.2	0.2/0.2	1.5/1.5	11.4/13.0	24.4	13.7	5.2	0.38	16.9	7.5	0.55	0.032	150	2094	192	213	120	333	CR,I
B61	1.0/1.8	0.5/0.5	1.5/1.8	10.5/15.5	26.0	14.3	5.1	0.37	20.7	7.7	0.55	0.036	150	2094	190	193	133	326	CR,I
B62	0.2/0.0	0.0/0.6	1.0/0.5	10.4/14.5	24.9	14.1	5.1	0.36	16.9	6.6	0.47	0.027	550	4978	195	236	195	431	I
B63	1.0/0.6	2.0/1.6	1.4/0.6	11.6/15.2	26.8	15.5	5.1	0.33	23.2	7.7	0.49	0.039	150	2094	191	196	144	340	CR,I
B64	0.6/0.5	1.0/0.5	1.5/1.0	10.3/10.7	20.9	13.9	5.2	0.37	20.5	6.5	0.47	0.023	650	5565	194	233	172	405	CR,I
B65	0.5/1.5	1.2/2.2	1.0/2.0	13.1/15.1	29.6	15.6	5.2	0.33	24.1	6.4	0.41	0.024	700	5847	197	260	192	452	CR,I
B66	1.0/0.5	1.2/1.0	0.5/1.2	12.4/10.8	23.2	15.1	5.1	0.35	19.1	7.1	0.48	0.032	250	2933	191	200	154	354	CR,I
B67	1.0/2.0	1.5/1.8	1.0/2.0	11.7/9.1	20.8	13.9	5.2	0.37	16.2	7.4	0.53	0.033	200	2536	192	210	140	350	CR,I
			Average	11.3/12	23.6	13.9	5.2	0.37	19.4	7.2	0.52	0.029	320	3319	192	215	145	360	
			Std dev	1.6/2.7	3.4	1.3	0.1	0.04	2.8	0.5	0.07	0.006	221	1531	2	22	35	63	

*Based on δ_a

TABLE XI. SUMMARY OF RESULTS FOR SERIES XIV

Test lubricant: O-67-22
Test disks: AMS 6260 (Batch B)
Break-in conditions: T_j = 90°F, V_s = 47 ips, V_t = 141 ips, 4 × 500(15)
Test conditions: T_j = 190°F, V_s = 450 ips, V_t = 1050 ips, 59(3), nitrogen environment

Test no	mm			Before break-in		At end of break-in			At failure										
	BBI	ABI	AT	δ_i/δ_{ji}, μin.	δ_{ji}, μin.	δ_a, μin.	h_m, μin	Λ_m	δ_f, μin	h_m, μin	Λ_{mf}*	l_f	P_f, lb	w_c, ppi	T_{p2}, °F	T_s, °F	ΔT_s, °F	T_{cr}, °F	Mode
B68	1.2/0 0	2 0/1.0	0 5/0 0	9.9/11.4	21.3	14.1	5.1	0 36	16 6	9 9	0 70	0 022	600	5276	195	240	151	391	CR,T
B69	0.8/1.0	1.0/1.5	0 5/0 5	9 1/14 1	23.2	14.3	5 1	0 36	18 8	10 8	0 76	0 023	250	2943	193	220	100	320	CR,T
B70	1.2/0 5	1.5/1.8	1 0/1.0	12.3/11 6	23 9	15.1	5.2	0 34	19.3	10 1	0 67	0 023	500	4672	194	230	143	373	CR,T
B72	3.0/2.0	3 2/2 5	2 0/1.8	11.2/11.9	23.1	16.1	5.1	0 32	20 4	10 8	0 67	0 019	300	3323	192	210	93	303	CR,T
B73	1.2/1.2	1.8/1.5	1.5/1 0	13.5/11.4	24.9	14 6	5 1	0 35	18 9	10 0	0 69	0 024	550	4978	194	230	155	385	CR,T
B76	1.0/1.5	1.2/1.0	1.0/0.5	13.0/10 0	23 0	13 6	5.5	0 40	19 1	10 4	0 76	0 018	400	4026	193	220	101	321	CR,T
B77	3.1/2.5	2 6/2.5	2.3/1.8	9.7/15.7	25.4	14.4	5.2	0 36	17 1	10 3	0 72	0 019	450	4355	193	220	112	330	CR,T
B78	1.6/1.2	1.5/2.0	1.0/2.0	8 4/5.8	14.2	13 0	5 2	0 40	17.2	10 2	0 79	0 019	500	4672	193	216	118	334	CR,T
B79	1 8/1.0	1.0/1 5	1.0/0 5	8 8/14.4	25.2	12 1	5 3	0 44	17 1	10 5	0 86	0 017	450	4355	191	200	99	299	CR,T
B80	0 5/0 5	1.5/1.2	0.5/0 5	10 4/11.1	21 5	14 6	5 3	0.36	18 9	9 8	0 67	0 020	550	4978	197	260	135	395	CR,T
			Average	10 6/11.7	22 4	14 2	5.2	0 37	18 3	10 3	0 73	0 020	455	4358	194	225	121	345	
			Std. dev	1 8/2.7	3.1	1.1	0 1	0 04	1 2	0 3	0 06	0 002	112	745	2	17	23	37	

*Based on δ_a.

TABLE XII. SUMMARY OF RESULTS FOR SERIES XV

Test lubricant: O-67-22
Test disks: AMS 6260 (Batch B)
Break-in conditions: T_j = 90°F, V_s = 47 ips, V_t = 141 ips, 4 × 500(15)
Test conditions: T_j = 190°F, V_s = 350 ips, V_t = 1050 ips, 50(3), belted drive

Test no	mm			Before break-in		At end of break-in			At failure										
	BBI	ABI	AT	δ_i/δ_{ji}, μin	δ_{ji}, μin	δ_a, μin	h_m, μin	Λ_m	δ_f, μin	h_m, μin	Λ_{mf}*	l_f	P_f, lb	w_c, ppi	T_{p2}, l	T_s, l	ΔT_s, l	T_{cr}, l	Mode
B81	1 0/1 8	1 7/2 0	1.5/2 1	8.3/11.8	20 1	16 2	5 3	0 33	46 1	9 9	0 61	0 023	650	5565	194	226	126	352	C R
B82	1.6/0 5	2 0/. 2	1.8/1 1	9.8/14.0	23.8	14 5	4 6	0 32	13 6	9 1	0 62	0 026	1150	8140	199	260	193	473	C R
B83	1.6/1 6	2 0/2 0	2 0/2 5	11 6/12 2	23 8	16 0	5.2	0 33	14 9	9 4	0 59	0 027	850	6655	197	260	169	429	C R
B84	2 0/0 0	1.8/0 6	1 3/0 5	11 2/9 4	20 6	15 1	5 3	0 35	14 0	9 5	0 63	0 025	800	6391	196	253	155	408	C R
B86	0.5/2 0	0 6/1 6	1 0/2 2	9 5/9 4	18 9	13 0	5 5	0 43	47 8	9 7	0 74	0 024	750	6122	196	246	142	388	C R
			Average	10.1/11 4	21 5	15 0	5 2	0 35	27 3	9 5	0 64	0 025	840	6575	196	253	157	410	
			Std dev	1 3/2 0	2 2	1.3	0 3	0 04	17 9	0 3	0 06	0 001	185	964	2	20	26	45	

*Based on δ_a

TABLE XIII. SUMMARY OF RESULTS FOR SERIES XVI

Test lubricant: O-67-22
Test disks: AMS 6260 (Batch B)
Break-in conditions: T_j = 90°F, V_S = 47 ips, V_t = 141 ips, 4 × 500(15)
Test conditions: T_j = 190°F, V_S = 450 ips, V_t = 1050 ips, 50(3), belted drive

Test no	mm			Before break-in		At end of break-in			At failure										
	BBI	ABI	AT	δ_1/δ_2, μin	δ_1, μin	δ_a, μin	h_m, μin	Δ_m	δ_f μin	h_m, μin	Δ_{mf}*	t_f	P_f, lb	w_e, ppi	T_{p2}, °F	T_s, °F	ΔT, °F	T_{cr}, °F	Mode
B87	2.0/1.0	2.2/1.6	1.5/1.0	11.0/12.6	23.6	15.5	5.5	0.35	15.4	9.6	0.62	0.025	650	5565	198	270	178	448	CR
B88	1.8/1.0	1.8/1.0	1.3/0.5	12.1/13.3	25.4	17.8	5.6	0.31	17.7	10.3	0.58	0.025	350	3683	196	253	134	387	CR
B89	1.0/0.0	2.0/1.5	2.0/1.5	9.1/17.9	27.5	19.2	5.5	0.28	18.0	10.0	0.52	0.026	350	3683	199	263	136	419	CR
B90	1.0/2.0	1.5/1.8	1.3/2.0	12.1/13.1	25.2	14.9	5.8	0.33	17.4	10.3	0.69	0.023	300	3323	197	263	113	376	C
B91	1.5/0.0	1.8/1.2	2.0/1.0	15.0/12.8	27.8	17.9	5.2	0.29	17.6	10.4	0.58	0.027	300	3323	196	253	131	384	
			Average	12.0/13.9	25.9	17.1	5.5	0.31	17.2	10.1	0.60	0.025	390	3915	197	264	138	423	
			Std dev	2.0/2.2	1.8	1.8	0.2	0.03	1.0	0.3	0.06	0.001	148	940	1	13	23	46	

*Based on δ_a

TABLE XIV. SUMMARY OF RESULTS FOR SERIES XVII

Test lubricant: O-67-22
Test disks: AMS 6260 (Batch B)
Break-in conditions: T_j = 90°F, V_S = 47 ips, V_t = 141 ips, 4 × 500(15)
Test conditions: T_j = 190°F, V_S = 350 ips, V_t = 817 ips, 50(3), belted drive

Test no	mm			Before break-in		At end of break-in			At failure										
	BBI	ABI	AT	δ_1, δ_2, μin	δ_1, μin	δ_a, μin	h_m, μin	Δ_m	δ_f μin	h_m, μin	Δ_{mf}*	t_f	P_f, lb	w_e, ppi	T_{p2}, °F	T_s, °F	ΔT, °F	T_{cr}, °F	Mode
B92	1.5/2.0	1.8/1.8	2.0/2.0	10.3/8.0	18.3	13.8	5.4	0.39	14.5	8.5	0.62	0.025	450	4755	195	236	130	366	CR
B93	2.6/1.5	2.0/1.5	3.0/2.0	17.6/10.5	26.1	16.4	5.8	0.35	16.7	8.5	0.52	0.029	400	4026	196	246	147	393	CR
B94	2.0/2.0	1.8/2.0	2.2/2.2	9.8/9.1	18.9	14.2	5.4	0.39	13.7	8.3	0.58	0.024	600	5276	198	243	146	389	CR
B95	2.5/2.2	1.3/2.4	2.5/2.6	12.2/9.6	21.8	15.8	6.2	0.39	15.7	9.2	0.58	0.028	200	2546	194	226	92	325	CR
B96	0.5/1.8	1.0/2.0	1.5/2.0	11.0/12.3	23.3	15.5	5.8	0.39	14.9	8.7	0.49	0.028	950	7167	201	290	218	508	CR
			Average	12.2/9.9	22.1	15.1	5.7	0.38	15.1	8.4	0.56	0.027	520	4634	196	248	148	396	
			Std dev	3.2/1.6	3.9	1.1	0.3	0.02	1.2	0.5	0.08	0.002	280	1708		28	44	68	

*Based on δ_a

TABLE XV. SUMMARY OF RESULTS FOR SERIES XVIII

Test lubricant: O-67-22
Test disks: AMS 6260 (Batch B)
Break-in conditions: T_j = 90°F, V_s = 47 ips, V_t = 141 ips, 4 × 500(15)
Test conditions: T_j = 190°F, V_s = 200 ips, V_t = 600 ips, 50(3), belted drive

Test no	mm,			Before break-in		At end of break-in			At failure										
	BBI	ABI	AT	δ_1/δ_2, μin	δ_{1r} μin	δ_a, μin.	h_m, μin	Λ_m	δ_f, μin	h_m, μin	Λ_{mf}*	f_f	P_f lb	w_e, ppi	$T_{\rho 2}$ l	T_v l	ΔT l	T_{cf} l	Mode
B97	0.5/2.0	1.0/1.5	1.8/2.0	13.7/12.3	26.0	16.6	5.2	0.31	16.5	5.8	0.35	0.033	1,850	11,176	201	303	234	537	CR
B98	0.5/1.0	1.0/1.3	1.5/1.8	10.3/10.7	21.0	17.1	5.2	0.30	16.8	6.6	0.38	0.030	750	6,122	195	240	135	375	CR
B99	0.0/1.2	0.5/1.0	1.0/1.5	12.7/10.2	22.9	17.5	5.2	0.29	17.0	6.7	0.38	0.033	650	5,565	195	236	138	374	CR
B100	1.5/1.5	1.8/1.5	1.5/1.5	12.3/10.5	22.6	13.6	5.2	0.32	16.1	6.5	0.48	0.035	800	6,391	196	250	163	413	CR
B101	0.0/1.0	0.5/1.0	1.0/1.5	10.2/13.3	23.5	16.5	5.6	0.33	16.1	6.2	0.37	0.031	1,300	8,833	197	260	183	443	CR
			Average	11.8/11.4	23.2	16.3	5.3	0.31	16.5	6.4	0.39	0.032	1,070	7,617	197	258	171	428	
			Std dev	1.5/1.3	1.8	1.5	0.2	0.01	0.4	0.4	0.05	0.002	503	2,350	3	27	40	67	

*Based on δ_2.

REFERENCES

1. Carper, H. J., Anderson, E. L., and Ku, P. M., "Development of the AFAPL Disk Tester for Gear Lubrication Research," AFAPL Technical Report 71-63, August 1971.

2. Blok, H., "Les temperatures des surface dans des conditions de graissage sous pression extreme," *Congr. mondial pétrole, 2 .ne Congr.*, Paris, Vol. 3, 1937.

3. Blok, H., "Theoretical Study of Temperature Rise at Surfaces of Actual Contact under Oiliness Lubricating Conditions," *Proc. Gen. Disc. on Lubrication*, I. Mech. E., 1937.

4. Dowson, D., "Elastohydrodynamic Lubrication," **Interdisciplinary Approach to the Lubrication of Concentrated Contacts**, P. M. Ku, editor, NASA SP-237, 1970.